



Mobile Pb-isotopes in Proterozoic sedimentary basins as guides for exploration of uranium deposits

Gregory J. Holk^{a,*}, T. Kurtis Kyser^b, Don Chipley^b, Eric E. Hiatt^c, Jim Marlatt^d

^aDepartment of Geological Sciences, California State University, Long Beach, 1250 Bellflower Blvd., Long Beach, CA 90840, USA

^bDepartment of Geological Sciences and Geological Engineering, Queen's University, Kingston, Ontario, Canada K7L 3N6

^cDepartment of Geological Sciences, University of Wisconsin, Oshkosh, 800 Algoma Blvd., Oshkosh, WI 54901-8649, USA

^dCameco Corp., 2121 11th St. W., Saskatoon, Saskatchewan, Canada

Received 15 May 2002; received in revised form 30 September 2002; accepted 25 December 2002

Abstract

Lead isotope ratios and associated trace element concentrations (U, Th and Pb) extracted by partial-leaching with 2% nitric acid from Proterozoic sandstones and basement rocks reveal much about the fluid evolution of sedimentary basins hosting unconformity-type uranium deposits. In addition, these techniques have great potential as a guide for exploration of uranium and other types of deposits in basins of any age. Isotope ratios of Pb in Proterozoic sandstones from basins known to contain high-grade uranium deposits are radiogenic at key geological localities and settings distal to known mineralization and particularly in altered zones proximal to mineralization. Sandstones completely cemented by quartz overgrowths typically have non-radiogenic Pb isotope ratios, indicating early closure of porosity and isolation of these rocks from later fluid events. Alternatively, the unconformity served as both a source of uranium and radiogenic Pb as well as an avenue for late-stage (<250–900 Ma) fluid flow. The mafic volcanic units, which are relatively reducing lithologies and therefore have removed uranium from basinal brines, have uranium-supported radiogenic Pb isotope ratios. Comparison of $^{238}\text{U}/^{206}\text{Pb}$ and $^{206}\text{Pb}/^{204}\text{Pb}$ ratios is useful in determining the timing and nature of U and Pb migration before, during and after mineralization in these basins. This comparison can be used to delineate the presence of radiogenic Pb isotope ratios that are not internally supported by uranium and thorium in rocks, eventually providing the explorationist with geochemical vectors that point toward sites of high potential for economic uranium mineralization.

© 2003 Elsevier B.V. All rights reserved.

Keywords: Unconformity-type uranium deposit; Partial leach techniques; Pb isotopes

1. Introduction

Numerous radiogenic isotope (Gulson and Mizon, 1980; Trocki et al., 1984; Miller et al., 1989; Pagel et al., 1993) and stable isotope (Kotzer and Kyser, 1995;

Fayek and Kyser, 1997; Renac et al., 2002) studies of ore and alteration minerals related to unconformity-type uranium deposits hosted by Proterozoic basins have shown that uranium ore bodies and associated alteration zones experience significant post-mineralization alteration and variable Pb loss during interaction with late-stage fluids. The migration and precipitation of radiogenic Pb from uranium-bearing ore bodies into

* Corresponding author. Fax: +1-562-985-8638.

E-mail address: gholk@csulb.edu (G.J. Holk).

the environs of these deposits provide an excellent opportunity to study the late-stage basinal fluid history as it relates to the remobilization of Pb, U and Th.

The purpose of this study is to determine the utility of Pb isotopes in the exploration for uranium deposits using high-resolution inductively coupled-plasma mass-spectrometry (HR-ICP-MS) coupled with partial leach extraction techniques of possible mobile metals (e.g., Hall, 1998; Goldberg, 1998; Mann et al., 1998). The rapid acquisition of Pb isotope data afforded by HR-ICP-MS makes an investigation like this feasible because the cost and time needed to analyze the required number of samples for the delineation of spatial Pb isotope trends are significantly reduced. Therefore, this technique may be a useful supplement to geophysical and other kinds of geochemical strategies already employed in mineral exploration. In addition, the isotopic composition of Pb mobilized from uranium-rich sources can also be used to evaluate where in these basins late fluid events occurred. Herein, we describe a set of Pb isotope ratios and concentrations from 270 sandstones and basement samples located at variable distances from known uranium deposits hosted by the McArthur Basin in Australia, the Athabasca Basin in Canada and the Thelon Basin in Nunavut, Canada.

2. Geologic considerations

2.1. The Kombolgie Sub-basin, northern Australia

The Kombolgie Basin in the Northern Territory of Australia is the northernmost part of the much larger Proterozoic McArthur Basin (Fig. 1). The McArthur Basin hosts numerous world-class unconformity-type uranium deposits of the Alligator Rivers Uranium Field as well as some of the world's largest sedimentary-hosted Pb–Zn–Ag deposits. The study area is located approximately 300 km east of Darwin on the Arnhemland Plateau. Samples from ten drill holes and an exposed silicified fault zone were analyzed for their Pb isotope compositions.

The Kombolgie Subgroup is the basal sequence of the terrestrial-to-marine Proterozoic Katherine River Group (Needham, 1988; Sweet et al., 1999). This flat-lying succession unconformably overlies gneissic Archean rocks and metasedimentary, metavolcanic and

intrusive Early Proterozoic rocks of the Pine Creek Geosyncline that were metamorphosed during the Barrimundi Orogeny between 1890 and 1870 Ma (Page and Williams, 1988) and the Top End Orogeny between 1870 and 1690 Ma (Needham, 1988). Included in the Pine Creek Geosyncline succession are schists of the Paleoproterozoic Cahill Formation, the host to most uranium deposits (Needham et al., 1988). The Kombolgie is comprised, in ascending stratigraphic order, of alluvial fan to braided stream facies of the Mamadawerre Formation, the mafic Nungbalgarri Volcanics, the fluvial-to-beach-to-eolian Gumarrimbang Formation, the felsic Gilruth Volcanics and the coastal-to-shallow marine Marlgoowa Formation (Fig. 1). Overlying the Marlgoowa are marine-facies glauconitic sandstones of the McKay Formation. Post-orogenic felsic intrusions of Jimbu Microgranite (Rawlings and Page, 1999) and mafic intrusions of Oenpelli Dolerite (Kyser et al., 2000) having ages of ca. 1720 Ma intruded the Kombolgie succession. This was followed by later magmatic events at 1370 and 1200 Ma that are marked by the intrusion of minor phonolitic and doleritic dikes (Page et al., 1980).

Uranium deposits of the Alligator Rivers Uranium Field occur just beneath the basal Kombolgie unconformity and are hosted by carbonaceous quartz-chlorite schist and chloritic rocks of the Cahill Formation or its stratigraphic equivalents (Needham, 1988). Within ore zones at Jabiluka, schists are brecciated with retrograde chlorite and sericite replacing the clast and matrix minerals as well as filling vein and breccia pore spaces (Binns et al., 1980). Except for the shear zone-hosted Nabarlek deposit, mineralization is stratigraphically controlled by variations in host-rock lithology and restricted to graphitic layers in schist. Strong chloritic alteration, dated at ca. 1380 Ma (Gulson and Mizon, 1980), and brecciation that overprints earlier silicification extends as much as 300 m above the unconformity in the Mamadawerre Formation at Jabiluka, indicating mineralization after the deposition of these sandstones (Gustafson and Curtis, 1983; Nutt, 1989). Primary mineralization at Koongarra, Jabiluka and Nabarlek occurred ca. 1640 Ma (Ludwig et al., 1987; Maas, 1989), at temperatures between 200 and 315 °C (Donnelly and Ferguson, 1980; Gustafson and Curtis, 1983; Wilde et al., 1989). Mineralization was associated with Ca–Mg rich saline (~ 25% Mg–CaCl₂) fluids (Durak et al., 1983; Wilde et al., 1989; Kyser

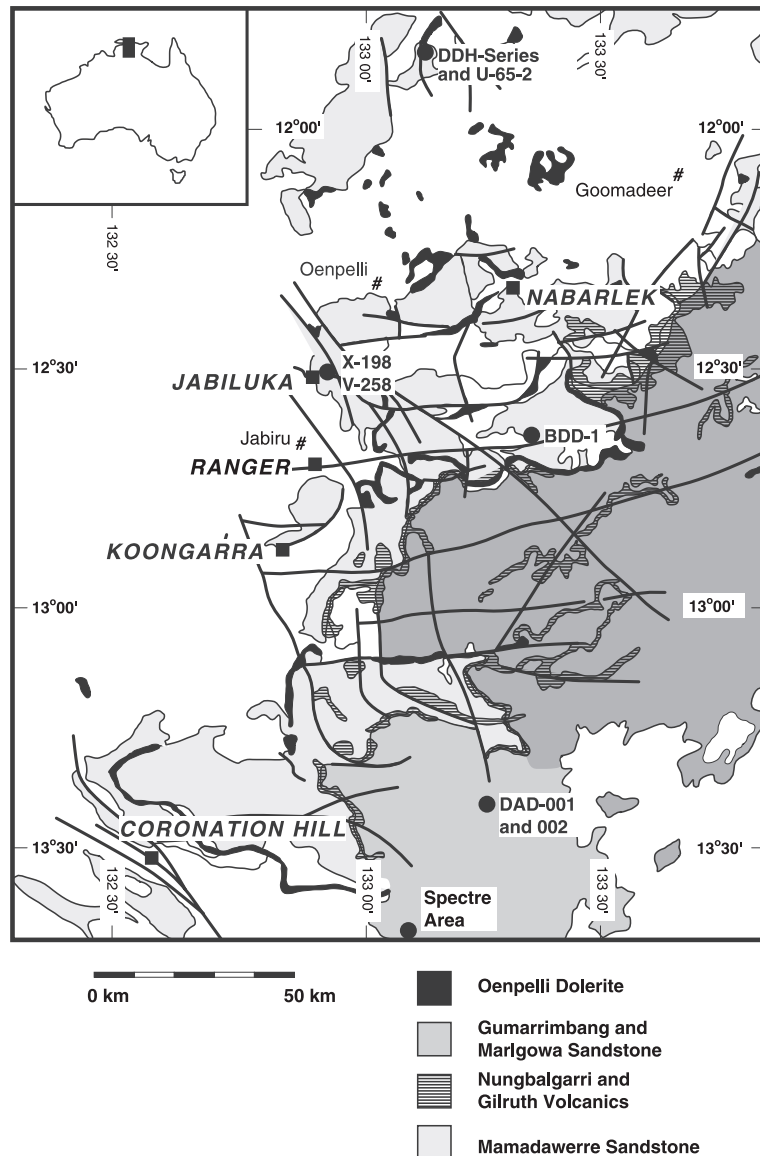


Fig. 1. Simplified geologic map of the Kombolgie Basin showing location and distribution of Kombolgie Subgroup sandstones and igneous rocks and the locations of major uranium deposits (solid squares) and drill holes studied from this area (solid circles). Basement plutonic and metamorphic rocks are indicated by white.

et al., 2000). A late U-mobilization event occurred between 600 and 400 Ma (Ludwig et al., 1987).

Sandstones in the Kombolgie Basin record a complex fluid history related to diagenesis, the intrusion of the Oenpelli Dolerite, and later tectonic events (Kyser et al., 2000). Porosity was significantly reduced by extensive silica cementation at 80–130 °C from low-

salinity (<10 wt.% NaCl) pore fluids during the earliest stage of diagenesis, especially in well-sorted lithologies. Peak diagenesis is marked by the filling of much of the remaining pore space with diagenetic 2M1 illite and near the unconformity or volcanic units, chlorite at ca. 200 °C from basinal brines. The intrusion of the Oenpelli Dolerite marks a major fluid event

involving saline (20–30 wt.% Na–Ca–Mg–Cl) basinal brines that resulted in quartz dissolution (250–400 °C) adjacent to the intrusion, quartz precipitation (<250 °C) near the intrusion, and numerous quartz veins and breccias distal to the dolerite. Later stages of the fluid evolution of the Kombolgie are related to faulting, fracturing and formation of quartz-rich veins as saline (22 wt.% Na–Ca–Mg–Cl) fluids were forced from deeper portions of the basin.

2.2. The Athabasca Basin

The Athabasca Basin, located in northern Saskatchewan, hosts the two largest high-grade uranium deposits in the world, Cigar Lake and McArthur River.

The crystalline basement that unconformably underlies the eastern part of the Athabasca Basin is part of the Cree Lake zone of the Churchill Province (Lewry and Sibbald, 1980). The Cree Lake Zone is divided into the Mudjatik, Wollaston, Peter Lake and Rottenstone domains (Fig. 2). Each of these domains represent high-grade metamorphism, anatexis and remobilization of Archean basement during the Hudsonian Orogeny (1900–1800 Ma). A well-developed paleosol extends several meters into the basement rocks just beneath the unconformity with the Athabasca Group. Numerous northwest trending 1280 Ma mafic dikes related to the Mackenzie dike swarm intruded along reactivated fracture zones (Armstrong and Ramaekers, 1985).

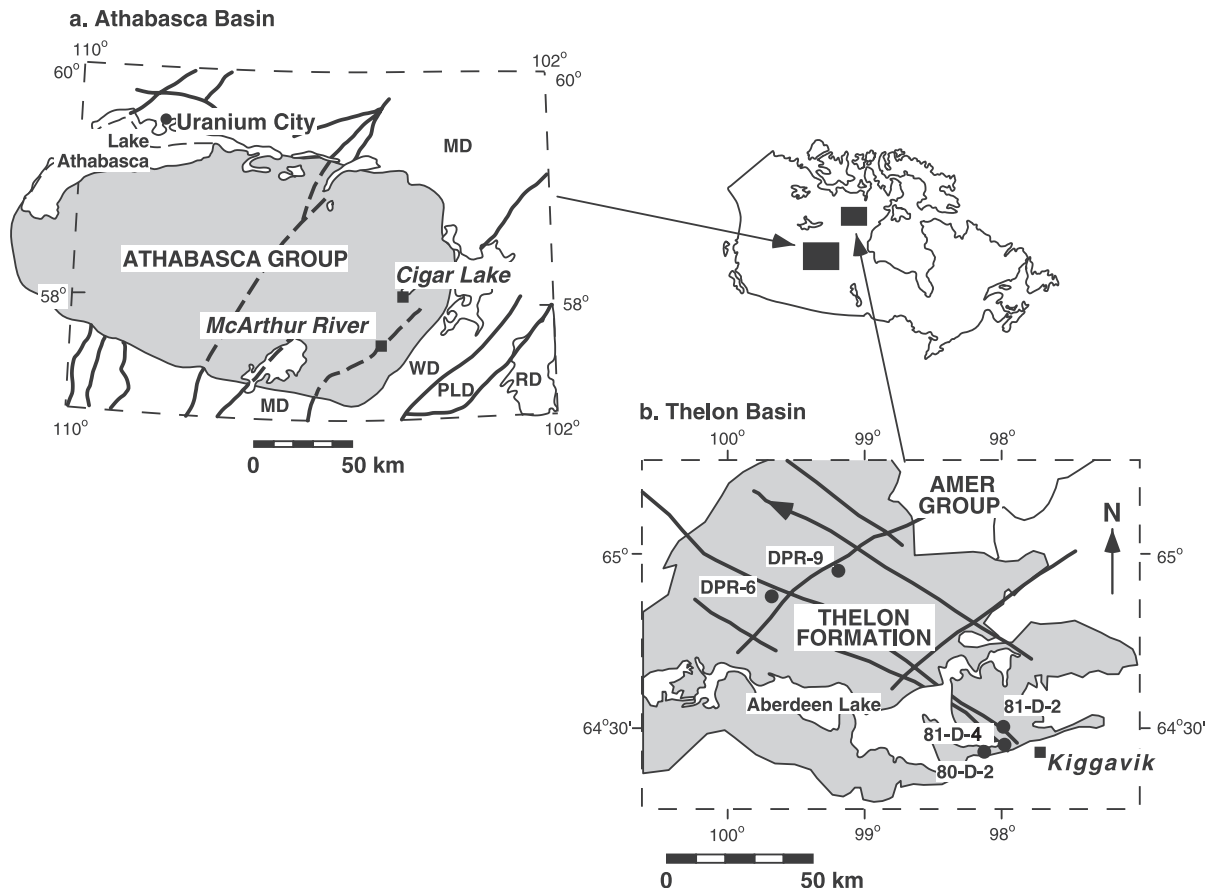


Fig. 2. Simplified geologic maps of the Canadian basins. (a) The Athabasca Basin (after Kotzer and Kyser, 1995) showing the locations of the Cigar Lake and McArthur River unconformity-type uranium deposits. Data from these deposits are shown in Figs. 6 and 7. The Mudjatik (MD), Wollaston (WD), Peter Lake (PLD) and Rottenstone (RD) lithostructural domains are indicated. (b) The northeastern Thelon Basin with locations of drill holes. Data from the Thelon Basin are described in Fig. 8.

The Athabasca Group is a 1–2-km thick succession composed primarily of fluvial sandstones and conglomerates (Ramaekers, 1981) with a minimum depositional age of 1740 Ma (Kyser et al., 2000). Permeable coarse-to fine-grained hematite-rich conglomerates and sandstones of the Manitou Falls and Fair Point Formations comprise the basal sequence of the Athabasca Group and these units are the focus of this study. The Manitou Falls Formation is comprised of basal coarse sandstone and conglomerate that grades into finer-grained sandstone with trough cross-bedding containing rare siltstone layers, abundant ripples, and mud rip-up clasts indicate a transition from an alluvial fan to a braided delta environment. Quartz comprises almost 100% of the detrital minerals in the Manitou Falls Formation, but there are rare occurrences of detrital muscovite and heavy minerals such as apatite and zircon. Unless cemented with quartz, these latter minerals are generally altered during diagenesis concurrent with basin evolution (Kotzer and Kyser, 1995; Kyser et al., 2000).

A complex fluid history related to diagenesis, mineralization and late-stage alteration is recorded in the Athabasca Basin (Kotzer and Kyser, 1995; Fayek and Kyser, 1997). Early-stage burial diagenesis of the Athabasca Group is marked by silica cementation at 150–170 °C (Kotzer and Kyser, 1995). Variable proportions of 2M illite and dickite produced by the alteration of detrital silicates characterize peak diagenesis in the basin. An assemblage consisting of hydrothermal illite and kaolinite intergrown with euhedral quartz and dravite, Al–Mg chlorite, and hematite occurs near faults, fractures, and ore deposits and represent hydrothermal alteration that occurred during the late stages of peak diagenesis and uranium deposition. Pore spaces of basal sandstones, conglomerates and metasedimentary rocks that straddle the unconformity are typically filled with chlorite. The presence of sudoite in fault zone up to 300 m above the unconformity indicates the migration of ore fluids into high stratigraphic levels (Kotzer and Kyser, 1995). Uranium deposition occurred at 1600–1700 Ma and was remobilized at ca. 900 and <400 Ma (Kyser et al., 2000).

2.3. The Thelon Basin

The Thelon Basin is located in the western part of Nunavut, Canada, between the Slave and Church-

ill geologic provinces. This basin hosts two minor uranium deposits, Kiggavik in the eastern part of the basin and Boomerang along the southwestern margin of the basin (Fig. 2; Gandhi, 1989). The Thelon Formation is a conglomerate-sandstone succession that is part of the Upper Dubawnt Group. These sediments unconformably overlie a basement complex that includes Archean orthogneiss, Paleoproterozoic metamorphic rocks of the Amer Group and the overlying Paleoproterozoic sedimentary and volcanic rocks of the Lower Dubawnt Group (Renac et al., 2002).

Most of the Thelon sandstones are quartz arenite to subarkose and have a very complex history of diagenesis in the eastern sub-basin that involves early phosphate cementation, quartz cementation as overgrowths on detrital quartz, formation of peak diagenetic illite and later infiltration of fluids that resulted in K-feldspar and chlorite replacement of the illite (Miller, 1983, Renac et al., 2002). Phosphate-rich units with anomalously high uranium concentrations (up to 640 ppm) occur as cement in association with detrital phosphate clasts and diagenetic illite and hematite, and are typically located near the base of the Thelon (Miller et al., 1989). There is a positive correlation between uranium and phosphorous concentration in these units (Miller and LeCheminant, 1981). Phosphates also occur as vein fillings in the Thelon Formation as well as in the regolith developed along the upper surface of the pre-Thelon erosional surface at the unconformity (Gall, 1994). The upper unit of the Thelon Formation is a succession of interlayered thinly bedded sandstone, siltstone, and mudstone capped by dolostone and siliceous dolostone. These lithologic trends indicate a transition from fluvial to marine depositional environment during deposition. The time of deposition is bracketed by the ages of the phosphate cement and a predepositional fluorite-bearing granite to be between 1720 and 1760 Ma (Miller and LeCheminant, 1981).

3. Analytical techniques

Approximately 10 cm³ of each sample was crushed using an aluminum jaw crusher and separated into two size fractions, 0.50–1.40 and 0.35–0.50 mm.

About 0.5 g of sample and 5 ml of 0.02 M HNO₃ spiked with ¹¹⁵In were loaded into a polyurethane tube, placed in an ultrasonic bath for 120 min and centrifuged. One gram of the liquid was diluted with 50 g of the spiked acid reagent and the Pb isotopic ratios and trace element concentrations were measured using a Finnigan MAT ELEMENT high-resolution ICP-MS.

The Pb isotope ratios were calculated using the signal intensities (counts/s) in low-resolution mode and have an average uncertainty of ca. 1% based on repeat analyses. Corrections were made for interferences from Hg and mass fractionation was monitored using Tl in the solutions and externally with in-house and NIST Pb isotope standards (NBS 981, normal Pb and NBS 983, radiogenic Pb). For each sample, ²⁰⁴Pb, ²⁰⁶Pb, ²⁰⁷Pb, ²⁰⁸Pb and ²⁰²Hg were measured, blank subtracted and ²⁰⁴Pb was corrected for ²⁰⁴Hg interference using ²⁰²Hg. Mass bias corrections were not applied as NIST standard values were near to certified values and well within the limits necessary in order to distinguish samples in the study. Concentrations were corrected for instrument drift and matrix using ¹¹⁵In as an internal standard and external calibration for element concentrations and blank subtraction.

A procedural blank and two in-house standards were analyzed during each run of 36 samples. The in-house standards represent two end-member isotopic compositions, with one having high radiogenic Pb and high trace element contents from a sandstone near the zone of intense hematite + kaolinite alteration from the immediate hanging wall of the Cigar Lake deposit (CL-231-421). The nonradiogenic standard is an unaltered sandstone distal to mineralization at Cigar Lake (CL-182-106.5). Leachate from the coarse fraction normally contained lower concentrations of U and Pb, but more radiogenic Pb than leachate from the finer size fraction (Table 1). The Pb from leaching of the coarse fraction is probably that adsorbed onto minerals during fluid migration events that occurred long after the main uranium mineralization event. The fine size fraction had a higher common Pb component that was probably leached from authigenic clay minerals and detrital minerals that were more exposed as a result of crushing. The larger concentrations of the common Pb component contained in the authigenic clay minerals and detrital

Table 1

Pb isotope ratios in coarse and fine fractions of sandstones proximal (CL-231-421) and distal (CL-182-106.5) to the Cigar Lake uranium deposit, Athabasca Basin

Sample	²⁰⁶ Pb/ ²⁰⁴ Pb	²⁰⁷ Pb/ ²⁰⁴ Pb	²⁰⁸ Pb/ ²⁰⁴ Pb	²⁰⁷ Pb/ ²⁰⁶ Pb	²⁰⁸ Pb/ ²⁰⁶ Pb
CL-231-421 coarse	131.00	21.09	73.47	0.16	0.56
CL-231-421 fine	111.27	20.02	66.47	0.18	0.59
CL-182-106.5 coarse	20.07	15.74	39.12	0.78	1.95
CL-182-106.5 fine	19.69	15.94	39.54	0.81	2.00

minerals effectively swamp out the radiogenic isotopic composition of the much less abundant Pb contained along grain boundaries. Except where indicated, data discussed in this paper are from the coarse size fraction.

4. Pb isotope systematics

Point-source concentrations of specific trace elements such as Pb, Co, Se, Sr and the isotopic fingerprint of daughter products from radioactive elements in unconformity-type uranium deposits provide an excellent means of determining the pathways of late-stage fluid migration in sedimentary basins that host these deposits. Most unconformity-type uranium deposits are enriched in trace elements such as Ni, Co, As, Cu, Pb and Th (e.g., Ruzicka, 1995) relative to basin fill or basement rocks in basins. In the case of uranium deposits, the decay of ²³⁸U and ²³⁵U results in the production of the daughter isotopes of ²⁰⁶Pb and ²⁰⁷Pb, respectively, at a known rate. In contrast, the concentration of ²⁰⁴Pb, the only stable isotope of Pb, is unchanged through time for a closed system. Thus, the ²⁰⁶Pb/²⁰⁴Pb and ²⁰⁷Pb/²⁰⁴Pb isotopic ratios provide information about the relative influence of ²³⁸U and ²³⁵U in a given rock system. Fig. 3 shows the isotopic evolution of ²⁰⁶Pb/²⁰⁴Pb in systems having initial ²³⁸U/²⁰⁶Pb ratios of 1000 and 100 for rock systems that formed at 1750, 1400, 900 and 400 Ma. Curves for the evolution of ²⁰⁷Pb/²⁰⁴Pb ratios with varying initial ²³⁵U/²⁰⁷Pb ratios would be similar, but we have chosen to use the ²³⁸U–²⁰⁶Pb system throughout this study because of the greater

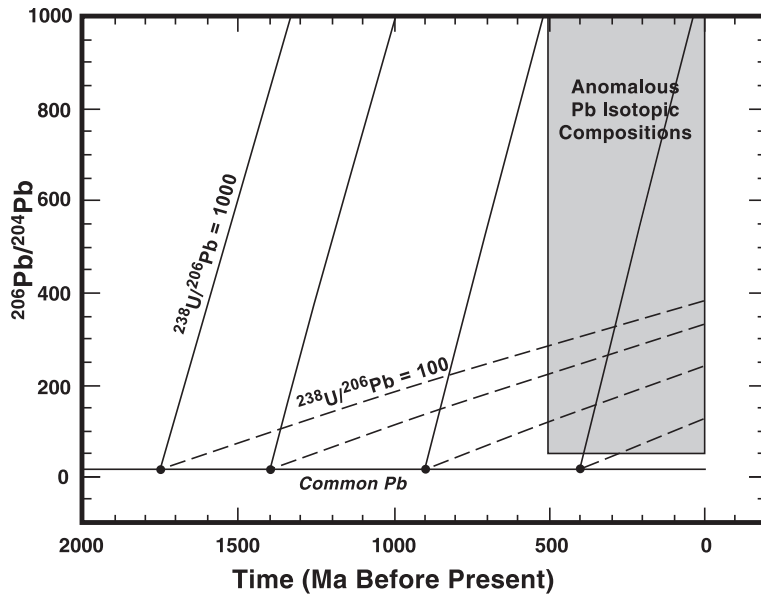


Fig. 3. Evolution of $^{206}\text{Pb}/^{204}\text{Pb}$ since 1750, 1400, 900 and 400 Ma for common Pb and rocks having initial $^{238}\text{U}/^{206}\text{Pb}$ of 1000 (solid curves) and 100 (dashed curves). Anomalous Pb isotopic compositions are considered to be those that are the product of mixing between common Pb and radiogenic Pb formed by the decay of uranium.

abundances of these isotopes. The 1750-Ma system represents the approximate age of deposition for the three sedimentary basins in this study and an upper limit for uranium ores (Kyser et al., 2000). The 1400-Ma system represents a major stage of uranium mineralization or recrystallization in the Athabasca (Baadsgaard et al., 1984; Philipe et al., 1993; Kotzer and Kyser, 1993) and Thelon (Miller et al., 1989) basins. Remobilization of uranium also appears to have occurred in the Alligator Rivers uranium field at this time (Gulson and Mizon, 1980; Ludwig et al., 1987). The 900-Ma system represents a major stage of uranium mobilization and mineralization recorded by many unconformity-type ore deposits (Hills and Richards, 1976; Philipe et al., 1993). The 400-Ma age is related to the late-stage fluid–rock interactions involving meteoric fluids and development of perched mineralization such as that at Cigar Lake (Philipe et al., 1993; Kyser et al., 2000) and late-stage alteration and isotopic disturbance at Ranger and Jabiluka (Hills and Richards, 1976; Ludwig et al., 1987). Episodes of Pb-mobilization from deposits in these Proterozoic basins may have been ongoing for at least 1000 Ma (Kyser et al., 2000).

The horizontal line at the bottom of Fig. 3 represents the evolution of common Pb based on the two-stage Pb evolution model of Stacey and Kramers (1975). Any $^{206}\text{Pb}/^{204}\text{Pb}$ ratio higher than the value for common Pb at a given time is radiogenic, but any $^{206}\text{Pb}/^{204}\text{Pb}$ ratio greater than 30 will be considered to be very radiogenic. These very radiogenic values are indicative of either late introduction of radiogenic lead into the rock by post-mineralization fluids or anomalously high U concentrations in the rock. Note that for an ore having an initial $^{238}\text{U}/^{206}\text{Pb}$ of 1000 and an initial common lead $^{206}\text{Pb}/^{204}\text{Pb}$ ratio, a $^{206}\text{Pb}/^{204}\text{Pb}$ of about 200 is reached only about 100 million years following the uranium mineralizing event. In contrast, the amount of time required for a system having $^{238}\text{U}/^{206}\text{Pb}=100$ to reach the same $^{206}\text{Pb}/^{204}\text{Pb}$ would be about 850 million years.

There are at least two ways for a rock to acquire radiogenic Pb isotopic compositions. A rock system can be closed such that internal decay of ^{238}U is the only source of new ^{206}Pb . In this case, the $^{206}\text{Pb}/^{204}\text{Pb}$ ratio of the rock gradually increases with the passage of time in a systematic fashion provided ^{206}Pb is not lost from the rock. A rock that has remained a closed

system with respect to uranium and Pb can be used as a geochronometer. Alternatively, a rock can obtain a radiogenic $^{206}\text{Pb}/^{204}\text{Pb}$ ratio by the incorporation of Pb transported by hydrothermal fluids that leached Pb decay products from a uranium-rich source. This is an open system with the potential to use the radiogenic Pb as a tracer to track the passage of fluids having a history of interaction with anomalous concentrations of uranium (e.g., an ore deposit). Therefore, if the concentrations of ^{238}U , ^{206}Pb , ^{204}Pb and the age of mineralization are known, the U–Pb isotopic system in basins can be used to delineate probable flow-paths for post-mineralization fluids.

To illustrate the potential of this technique, consider an unconformity-type uranium deposit that formed at ca. 1400 Ma. Radioactive decay of ^{238}U to ^{206}Pb and ^{235}U to ^{207}Pb should result in a 20% conversion of U to Pb over 1200 million years. However, much lower Pb concentrations are found in uraninite from unconformity-type deposits of this age and virtually all samples from various deposits have significantly discordant U–Pb ages (e.g., Trocki et al., 1984; Kotzer and Kyser, 1991, 1993; Fayek and Kyser, 1997). Significant Pb loss has occurred from ore during interaction with later fluids, most likely at ca. 300–400 Ma (Wilson et al., 1987; Kotzer and Kyser, 1991, 1993, 1995). For example, as much as ~ 25 million kilograms of Pb having $^{206}\text{Pb}/^{204}\text{Pb}$ and $^{207}\text{Pb}/^{204}\text{Pb}$ ratios >10,000 may have been mobilized away from the 180 million kilogram McArthur River deposit (Cameco Corporation, 1997) in the Athabasca Basin by these fluids that affected the deposit >1000 million years after mineralization. If this Pb were precipitated in portions of the fluid system “downstream” from this ore body, there would be an extremely radiogenic legacy in the rocks provided there is a small concentration of common Pb in most of the rocks around the deposit prior to fluid infiltration. This is shown to be true at the nearby Cigar Lake deposit where metapelitic gneisses proximal to the orebody have highly radiogenic $^{206}\text{Pb}/^{204}\text{Pb}$ ratios that range from 19.8 to 285.7, with most values being much greater than the typical crustal values of ~ 19 (Pagel et al., 1993). To date, no studies have determined the extent of radiogenic Pb migration into either basement or sandstone rocks distal to unconformity-type uranium deposits.

5. Results

5.1. The Kombolgie Sub-basin, northern Australia

5.1.1. King River area

Four shallow drill holes that traverse sandstones, schist and the Oenpelli Dolerite in the King River area of the northern Kombolgie Basin (Fig. 1), which together represent the general stratigraphy in the area, were analyzed for Pb isotope ratios (Fig. 4). These data allow assessment of the influence of the Oenpelli Dolerite as a local reductant for uranium, which could subsequently result in mobile radiogenic Pb isotope ratios that resemble those associated with economic uranium deposits. Kyser et al. (2000) have reported that basinal brines extensively altered the Oenpelli Dolerite during the evolution of the basin and the Oenpelli Dolerite would have acted as a reductant for any dissolved uranium.

All samples from the Mamadawerre Formation have $^{206}\text{Pb}/^{204}\text{Pb}$ ratios greater than common Pb (Fig. 4). The two samples from DDH-243 also have very radiogenic $^{208}\text{Pb}/^{204}\text{Pb}$ ratios (167.22 and 179.53) and high ^{232}Th concentrations (400–7000 ppb), indicating significant Th-derived ^{208}Pb . Quartz-cemented sandstones adjacent to the Oenpelli Dolerite in DDH 244 have variable $^{206}\text{Pb}/^{204}\text{Pb}$ ratios (25.09–90.14). Samples with the highest $^{206}\text{Pb}/^{204}\text{Pb}$ ratios (191.79–2579.7) include sandstones closest to the dolerite and the altered dolerites themselves. Uranium concentrations in these rocks are very high (26–1137 ppm) and are as much as 30 times greater than that for Pb, indicating much of the radiogenic Pb is produced in situ. These samples have $^{207}\text{Pb}/^{206}\text{Pb}$ ratios of less than 0.100, so that the initial U/Pb of the source of the radiogenic Pb was greater than 1000. In contrast, $^{208}\text{Pb}/^{204}\text{Pb}$ ratios for these samples are not very radiogenic (48.90–76.67) and less altered dolerites farther from the contact have much less radiogenic $^{206}\text{Pb}/^{204}\text{Pb}$ ratios (35.71 and 64.36) as well as much lower uranium concentrations (1625 and 2724 ppb). The schist from the Cahill Formation at the contact with the Oenpelli Dolerite in DDH-241 has a very radiogenic $^{206}\text{Pb}/^{204}\text{Pb}$ ratio of 547.78 and $^{208}\text{Pb}/^{204}\text{Pb}$ ratio of 439.67. Surface outcrop samples from the King River area have $^{206}\text{Pb}/^{204}\text{Pb}$ ratios near that of modern common Pb (18.15–25.00).

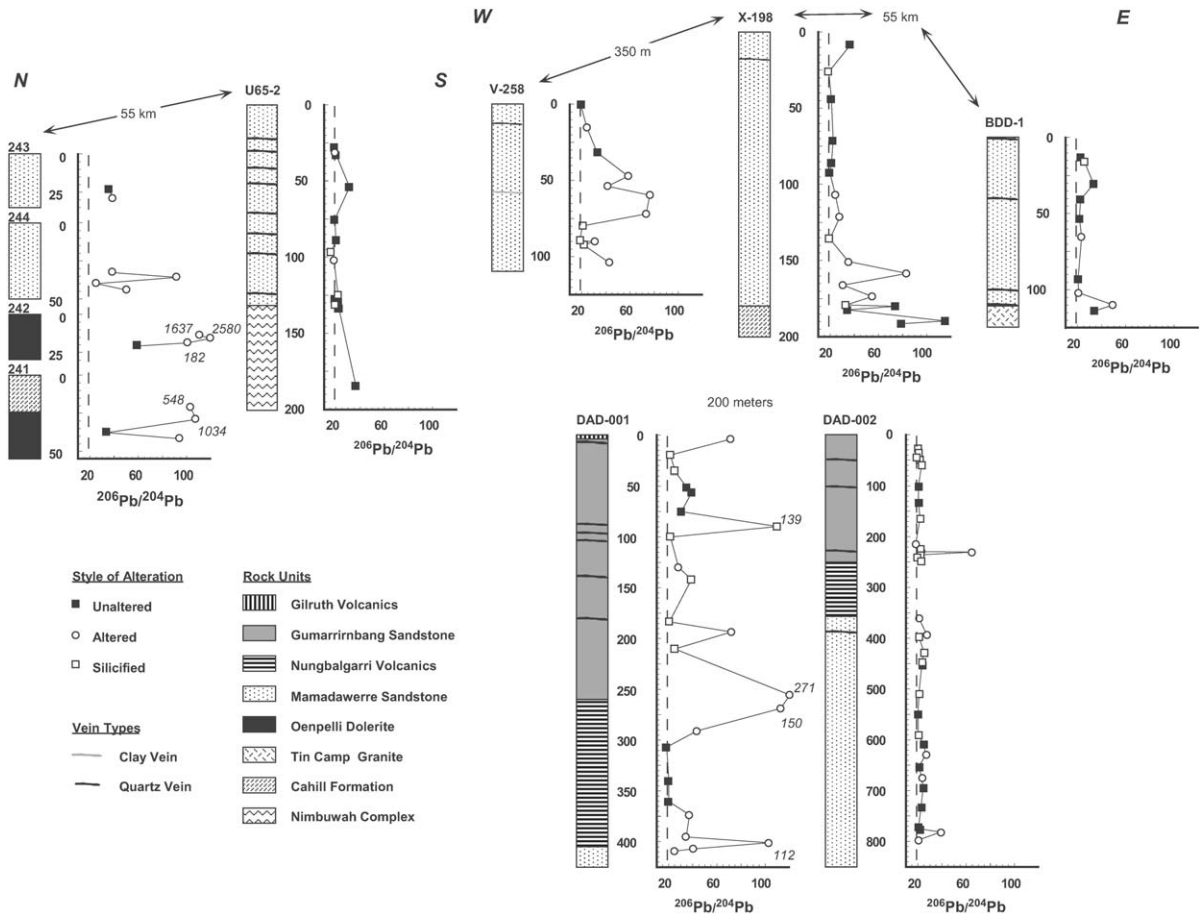


Fig. 4. $^{206}\text{Pb}/^{204}\text{Pb}$ ratios versus depth from drill holes that cut portions of the Komolgie Subgroup in the northern McArthur Basin, Australia. These include: Four short holes that traverse the unconformity in the King River area (DDH-series recombined stratigraphically as shown). A heavily veined sequence of Mamadawerre sandstone a few kilometers south of the Nabarlek deposit (U-65-2). Altered Mamadawerre sandstone near mineralization at Jabiluka (V-258 and X-198). A sequence of silicified Mamadawerre sandstone near the Beatrice Inlier (BDD-1). A thick section through the Gumarrirbang sandstone, the Nungbalgarri Volcanics and the Mamadawerre sandstone from two holes (DAD-001 and DAD-002) drilled into the southern part of the basin. Shown are unaltered lithologies (solid squares), silicified sandstones (open squares) and altered sandstones, dolerite and schist (open dots). The dashed line at $^{206}\text{Pb}/^{204}\text{Pb} = 18.700$ represents modern common Pb (Stacey and Kramers, 1975).

Drillhole U-65-2 (Fig. 4) samples a 129-m long section of heavily fractured and quartz-veined section of Mamadawerre Formation within the King River area north of the Nabarlek deposit. Most $^{206}\text{Pb}/^{204}\text{Pb}$ ratios in the sandstone are non-radiogenic (17.70–22.49), although one sample from a fracture zone 75 m above the unconformity has a slightly radiogenic $^{206}\text{Pb}/^{204}\text{Pb}$ ratio of 31.52. All quartz-cemented sandstones have $^{206}\text{Pb}/^{204}\text{Pb}$ ratios within analytical error of common Pb and very low concentrations of

uranium (<60 ppb). Cahill-equivalent schist at the unconformity has a remarkably non-radiogenic $^{206}\text{Pb}/^{204}\text{Pb}$ ratio of 21.06, indicating no movement of fluids transporting radiogenic Pb through this zone. A schist located 54 m below the unconformity has a slightly elevated $^{206}\text{Pb}/^{204}\text{Pb}$ value of 36.37 and a uranium concentration of 492 ppb. All the slightly radiogenic samples have low $^{238}\text{U}/^{206}\text{Pb}$ ratios indicative of the introduction of radiogenic Pb into these rocks.

5.1.2. Jabiluka

Samples from two drill holes near the Jabiluka uranium deposit were studied for the purpose of comparing isotopic and elemental distributions proximal and distal to known mineralization. Hole X-198 samples a 182-m thick section of the lowermost Mamadawerre sandstone just above the mineralized zone and hole V-258 samples 107 m of heavily altered, desilicified and chloritized lowermost Mamadawerre Formation approximately 350 m east of X-198 (Fig. 4).

From the surface down to 35 m above the unconformity in X-198, the $^{206}\text{Pb}/^{204}\text{Pb}$ ratios of relatively unaltered and silicified sandstone are close to those of common Pb (18.25–27.65; Fig. 4). The chloritized and desilicified lowermost 35 m of section have more variable $^{206}\text{Pb}/^{204}\text{Pb}$ ratios (31.64–83.75) and low U concentrations (<100 ppb), suggesting the late introduction of radiogenic Pb from the ore deposit beneath this section. However, the $^{208}\text{Pb}/^{204}\text{Pb}$ ratios of these altered sandstones are also very radiogenic (59.79–245.68). One silicified sandstone within a meter of the unconformity has a $^{206}\text{Pb}/^{204}\text{Pb}$ ratio of 33.71, much less than those of the overlying altered rocks, indicating that even sandstones proximal to the ore can be sealed from the effects of later fluids by early quartz cementation. A weathered kaolinite-bearing sandstone 8 m below the surface has a $^{206}\text{Pb}/^{204}\text{Pb}$ ratio of 36.55, perhaps due to radiogenic Pb and U accumulation near the surface, similar to that described by Von Gunten et al. (1999) at the nearby Ranger deposit. The coarse fraction of these sandstones typically has more radiogenic Pb isotope ratios than the fine size fraction. This is likely a product of preferential concentration of the uranium-sourced Pb onto grain boundaries of coarse sand grains as opposed to the common Pb fraction being concentrated in detrital grains.

The $^{206}\text{Pb}/^{204}\text{Pb}$ ratio (112.5) of a slightly mineralized (U = 1470 ppb) graphitic schist 10 m below the unconformity is radiogenic. Non-mineralized schists have less radiogenic and more variable $^{206}\text{Pb}/^{204}\text{Pb}$ ratios (34.57–79.58). High $^{206}\text{Pb}/^{204}\text{Pb}$ ratios accompanied by low $^{238}\text{U}/^{206}\text{Pb}$ ratios are consistent with the introduction of radiogenic Pb into these altered Cahill schists. There appears to be no difference between the Pb isotope ratios of the fine and coarse size fractions for the basement schists.

Although it is further from mineralization, the degree of chloritic alteration and desilicification in V-258 is much more intense than that observed in X-198. Desilicified sandstones normally have radiogenic $^{206}\text{Pb}/^{204}\text{Pb}$ ratios (30.98–76.55), with the most radiogenic values associated with the late clay-filled veins. However, one sample of weathered sandstone with kaolinite replacing illite near the surface has a non-radiogenic $^{206}\text{Pb}/^{204}\text{Pb}$ ratio (23.70). As before, quartz-cemented sandstones have relatively non-radiogenic $^{206}\text{Pb}/^{204}\text{Pb}$ ratios. In this hole, quartz-cemented sandstones occur interlayered between two desilicified zones of intense chloritic and illitic alteration; thus, these silicified zones may have been barriers to the movement of late-stage fluids. Similar to the altered Cahill Schists, low $^{238}\text{U}/^{206}\text{Pb}$ ratios in association with radiogenic $^{206}\text{Pb}/^{204}\text{Pb}$ ratios in the sandstones at Jabiluka indicate the addition of radiogenic Pb.

5.1.3. The Ranger Fault-Beatrice Inlier

Drill hole BDD-1 contains a heavily fractured, quartz-cemented section of Mamadawerre sandstone with late-stage kaolinite alteration. $^{206}\text{Pb}/^{204}\text{Pb}$ ratios between 20.62 and 25.13 for most of these sandstones indicate only limited migration of radiogenic Pb through these rocks (Fig. 4). The Tin Camp Granite in the basement ($^{206}\text{Pb}/^{204}\text{Pb}$ = 33.75) and sandstone ($^{206}\text{Pb}/^{204}\text{Pb}$ = 49.26) near the unconformity have only slightly radiogenic $^{206}\text{Pb}/^{204}\text{Pb}$ and $^{207}\text{Pb}/^{204}\text{Pb}$ ratios. Except at the unconformity, U and Pb concentrations are all below 100 ppb and the coarse fractions are only slightly more radiogenic than the fine size fractions. There is no correlation between the degree of fracturing and $^{206}\text{Pb}/^{204}\text{Pb}$ ratios in this section.

5.1.4. Southern Kombolgie Basin

Two drill holes (DAD-001 and DAD-002) located in the southern Kombolgie Sub-basin (Fig. 1) that traverse the Kombolgie section from the Gilruth volcanic member down to conglomerates of the Mamadawerre Formation were studied. In addition, two samples of Gumarrimbang Formation, one sample of Margowa Formation, and two samples of McKay Formation from other parts of the basin were also studied.

The $^{206}\text{Pb}/^{204}\text{Pb}$ and $^{207}\text{Pb}/^{204}\text{Pb}$ ratios in the extensively fractured DAD-001 (Fig. 4) are variable with the most radiogenic ratios in sandstones proximal to volcanic units and fractures that cut zones with abun-

dant quartz cements. The Gumarrirbang sandstone is highly variable in $^{206}\text{Pb}/^{204}\text{Pb}$ ratios, ranging between 21.07 and 271.18, but most samples have elevated $^{206}\text{Pb}/^{204}\text{Pb}$ relative to modern common Pb. Uranium concentrations are also highly variable, but samples with the highest concentrations (2750–9550 ppb) are fractured and silicified with coarse hematite crystals with radiogenic $^{206}\text{Pb}/^{204}\text{Pb}$ ratios (>71.19). Fractured Gumarrirbang sandstone nearest to the Nungbalgarri volcanic rocks have the highest $^{206}\text{Pb}/^{204}\text{Pb}$ ratios (up to 271.18). Most sandstone with abundant quartz cement have nonradiogenic $^{206}\text{Pb}/^{204}\text{Pb}$ ratios (21.07–25.64), whereas more porous sandstones have slightly radiogenic $^{206}\text{Pb}/^{204}\text{Pb}$ ratios (32.98–39.14). Drusy quartz-filled fracture zones have very radiogenic $^{206}\text{Pb}/^{204}\text{Pb}$ ratios (39.05–139.33), indicating that these fractures served as pathways for the transport of radiogenic Pb. The source of this radiogenic Pb was likely local because nearby altered Nungbalgarri volcanic rocks have very radiogenic $^{206}\text{Pb}/^{204}\text{Pb}$ ratios (35.74–150.80) and high U concentrations (650–6940 ppb). Unaltered basalt flows in the middle of the Nungbalgarri section have nonradiogenic $^{206}\text{Pb}/^{204}\text{Pb}$ ratios (18.26–20.54) as well as low U concentrations (<200 ppb). Coarse fraction samples typically have higher $^{206}\text{Pb}/^{204}\text{Pb}$ and $^{207}\text{Pb}/^{204}\text{Pb}$ ratios and lower Pb concentrations. $^{208}\text{Pb}/^{204}\text{Pb}$ ratios from this hole are also variable, but generally not very radiogenic.

This contrasts with sections of the Gumarrirbang and Mamadawerre from the less-fractured drillhole DAD-002 that have remarkably uniform and non-radiogenic $^{206}\text{Pb}/^{204}\text{Pb}$ ratios (18.57–26.90). Concentrations of leachable U throughout this hole are also very low (<200 ppb) except for a sample of Gumarrirbang sandstone with minor quartz cement, lots of pore-filling illite, solution cavities and late-stage bypyramidal quartz 10 m above the Nungbalgarri contact. This sample has a $^{206}\text{Pb}/^{204}\text{Pb}$ of 65.05 and U=257 ppb. Another exception is a sample of conglomeratic Mamadawerre Formation containing volcanic pebbles near the bottom of the hole with a $^{206}\text{Pb}/^{204}\text{Pb}$ ratio of 38.21.

5.1.5. Spectre area

The Spectre area is located in the southernmost part of the Kombolgie Sub-basin (Fig. 1). Reconnaissance surveys conducted by Cameco Australia discov-

ered a small showing of uranium mineralization hosted by a small fault splay associated with a major silicified fault along strike of the South Alligator trend of mineralization. Rock units in this area are divided into silicified fault breccia, unsilicified Marlgowa sandstone and McKay sandstone. Sites of uranium mineralization occur sporadically adjacent to silicified zones in the sandstones.

An east–west traverse across a silicified brecciated sinistral fault zone was collected at the Spectre locality (Fig. 5). Thin quartz veins that fill fractures cut many of these silicified sandstones. The fault is near-vertical and the associated silicified breccia zone is up to 200 m thick. Secondary fault splays are oriented east–west. Mineralization is associated with late-stage drusy quartz veins that cut unsilicified brecciated sandstone. Breccia fillings are pink while clasts are bleached and silicified.

Most silicified and brecciated sandstones of the fault zone have $^{206}\text{Pb}/^{204}\text{Pb}$ (18.93–20.23), $^{207}\text{Pb}/^{204}\text{Pb}$ (15.69–16.51) and $^{208}\text{Pb}/^{204}\text{Pb}$ (38.12–39.44) ratios indicative of common Pb. Most of the Marlgowa Formation samples also have remarkably unradiogenic $^{206}\text{Pb}/^{204}\text{Pb}$ (18.85–21.52), $^{207}\text{Pb}/^{204}\text{Pb}$ (15.71–16.06) and $^{208}\text{Pb}/^{204}\text{Pb}$ (37.20–38.53) ratios. As expected, one mineralized sample has extremely high $^{206}\text{Pb}/^{204}\text{Pb}$ (833.57) and $^{207}\text{Pb}/^{204}\text{Pb}$ (76.45) ratios and slightly elevated $^{208}\text{Pb}/^{204}\text{Pb}$ (40.59) ratio. The absence of fault-related silicified sandstones with radiogenic Pb isotope ratios indicates either that permeability along this fault has been restricted since emplacement of any uranium mineralization or that there is no significant mineralization in the area.

Except near mineralization, total leachable Pb concentrations are all less than 1000 ppb (Table 2). The three samples proximal to mineralization have total Pb concentrations of 1377, 5835 and 9670 ppb. Leachable U concentrations are very low (<50 ppb) for most of the silicified fault breccias, although two breccias near a mineralized zone have higher U concentrations (394 and 2204 ppb). Evidence for later migration of radiogenic Pb or other elements is lacking in this area.

5.2. The Athabasca Basin

5.2.1. Cigar Lake

The Cigar Lake deposit (Fig. 2a) is hosted by Paleoproterozoic Athabasca sandstones and is situated

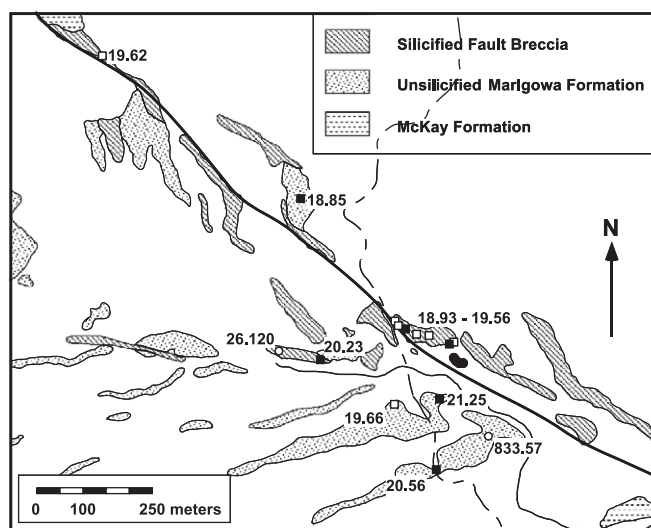


Fig. 5. Simplified geologic map of a silicified NW–SE-trending fault zone in the southernmost Komolgie Basin at the Spectre locality. $^{206}\text{Pb}/^{204}\text{Pb}$ values of silicified fault breccia (open boxes), unsilicified Marglowa Formation (closed boxes) and mineralized veins (open dots) are shown. Map courtesy of D. Thomas (Cameco).

along the unconformity with Paleoproterozoic basement rocks. Average grades are 7.9% U_3O_8 and reserves are estimated to be 150,000 tons (Bruneton, 1993). The orebody is approximately 130 m below the surface and lies on deformed graphitic metapelite. Perched ore bodies of secondary mineralization occur about 300 m above the unconformity in sandstones deformed by late faults. Alteration at Cigar Lake is characterized by a hematite and an illite zone proximal to the ore zone surrounded by a kaolinitic zone of unconsolidated sand encased by an outer zone of silicification (Fouques et al., 1986).

$^{206}\text{Pb}/^{204}\text{Pb}$ (and $^{207}\text{Pb}/^{204}\text{Pb}$ and $^{208}\text{Pb}/^{204}\text{Pb}$) ratios from drill holes near Cigar Lake show numerous systematic trends (Fig. 6). These data are summarized in Table 3. Extensive late-stage migration of fluids along the unconformity is indicated by radiogenic Pb isotope ratios ($^{206}\text{Pb}/^{204}\text{Pb} = 56.52\text{--}194.80$) both near and away from the orebody. The relatively non-radiogenic character of silicified sandstones ($^{206}\text{Pb}/^{204}\text{Pb} = 19.58\text{--}36.75$) is similar to our observations at Jabiluka. This is consistent with these silicified zones being aquitards during late Pb-mobilization events, although a slight amount of radiogenic Pb was introduced into the silicified sandstones directly above the deposit. Most of the radiogenic

samples have low $^{238}\text{U}/^{206}\text{Pb}$ and high $^{206}\text{Pb}/^{204}\text{Pb}$ ratios indicative of the Pb being derived from decay of early-stage uranium mineralization not currently in the sample. A systematic increase in all Pb isotope ratios toward more radiogenic values in a downward direction through a desilicified section of the Manitou Falls Formation immediately above the Cigar Lake deposit suggests that these highly altered rocks were permeable to later fluids that transported radiogenic Pb. Leachable Pb increases with more radiogenic isotopic ratios in these sandstones, but this correlation is absent in the basement rocks. Most sandstones from CL-229, only 325 m northeast of mineralization, have mostly nonradiogenic Pb isotope ratios.

5.3. McArthur River

The McArthur River uranium deposit is the largest and highest grade uranium deposit in the world with total reserves and resources of 190 million kilograms U_3O_8 and average grades of 15% U_3O_8 (Cameco Corporation Annual Report, 1997). Mineralization is fault-hosted in graphitic metapelite of the Paleoproterozoic Wollaston Group and basal sandstones of the Paleoproterozoic Athabasca Group at the unconformity-

Table 2

Ranges in Pb isotopic compositions and concentrations of Pb, Th and U (ppm) in leachates of coarse and fine fractions of sandstones from various areas of the Kombolgie Basin

Study area	Formation	No. samples	$^{206}\text{Pb}/^{204}\text{Pb}$	$^{207}\text{Pb}/^{204}\text{Pb}$	$^{208}\text{Pb}/^{204}\text{Pb}$	$^{207}\text{Pb}/^{206}\text{Pb}$	$^{208}\text{Pb}/^{206}\text{Pb}$	Pb	Th	U	Alteration
South Horn	Mamadawerre	2	20.57–24.91	16.89–16.76	49.10–51.47	0.67–0.82	1.97–2.51	228–289	187–314	135–139	desilicified
Beatrice Fault	Mamadawerre	1	25.14	20.99	53.43	0.84	2.13	69	6.5	10.8	silicified
		5	20.63–33.30	16.57–19.20	48.23–52.20	0.53–0.87	1.57–2.40	31–140	35–200	31352.0	un(de)silicified
		3	20.78–49.27	15.19–18.36	49.60–122.53	0.37–0.76	2.39–2.49	78–403	95–899	30–638	desilicified
	Granite	1	33.76	17.77	132.60	0.53	3.93	661	1406	212	
Ranger	Mamadawerre	2	23.04–27.10	15.61–17.91	40.12–49.95	0.66–0.68	1.84–1.85	20029	215–572	110–158	desilicified
Near	Mamadawerre	3	19.92–22.04	16.71–17.33	42.35–50.06	0.78–0.84	1.71–2.28	60–91	41–242	14–56	silicified
Nabarlek		8	18.61–31.53	15.02–18.02	42.18–61.95	0.56–0.91	1.96–2.41	41–211	42–268	14–61	un(de)silicified
		2	17.71–19.65	16.08–16.91	45.96–41.17	0.86–0.91	2.33–2.35	65–129	53–112	16–17	desilicified
	Cahill	2	21.07–36.37	16.79–17.85	59.00–71.41	0.80–0.49	1.96–2.81	71–819	19–492	19–492	schist
King River	Mamadawerre	4	18.16–36.03	13.85–17.60	38.54–167.27	0.49–0.81	1.88–4.64	25–911	130–7186	4.5–214	un(de)silicified
		6	25.10–90.14	18.93–33.60	75.15–179.54	0.34–0.78	1.32–4.76	68–352	128–6227	81–318	desilicified
	Cahill	1	547.78	67.90	439.67	0.12	0.81	329	4192	43437	schist
	Oenpelli	4	181.80–2579.77	20.55–229.12	48.91–89.15	0.08–0.11	0.02–0.30	234–3680	42–5499	26020–1137338	altered
		3	35.02–94.13	17.30–22.99	47.55–60.46	0.24–0.49	0.64–1.36	294–4366	80–190	366–1876	slightly altered
Jabiluka	Mamadawerre	2	18.24–36.55	17.18–17.56	41.24–47.38	0.54–0.94	1.28–2.60	3.8–206	16–274	76	weathered
		6	18.26–33.71	16.36–17.36	39.45–68.95	0.52–0.90	1.98–3.26	97–228	9.1–288	5.1–94	silicified
		5	20.10–33.67	16.22–18.50	40.11–61.87	0.55–0.82	1.84–2.09	53–259	7.3–265	4.5–109	un(de)silicified
		13	23.71–83.75	16.30–22.96	43.10–245.69	0.26–0.72	0.88–3.36	67–503	5.4–1207	4.7–571	desilicified
	Cahill	3	34.58–112.54	17.43–23.79	53.67–196.31	0.21–0.51	0.48–4.34	181–616	15–721	39–1469	schist
Deaf Adder	McKay	3	19.91–21.26	15.90–16.07	37.20–43.82	0.75–0.80	1.75–2.20	98–426	27–286	103–215	silicified
		1	28.88	16.86	44.34	0.59	1.55	217	189	72	desilicified
	Rhyolite	1	24.04	16.38	44.00	0.68	1.83	303	200	773	
	Marlgowa	8	18.94–19.67	15.69–16.54	38.25–40.45	0.80–0.87	1.95–2.13	172–365	1.9–29	5.9–96	silicified
		2	18.85–19.23	15.72–15.75	38.13–38.54	0.82–0.84	1.98–2.04	158–167	3.8–15.4	6.2–8.3	unaltered
		4	19.32–833.58	15.74–76.46	38.55–40.60	0.09–0.82	0.05–1.99	76–4942	19–779	4.7–51898	desilicified
	Gumarrimbang	17	19.79–25.65	15.26–16.92	36.08–71.85	0.64–0.80	1.51–2.80	140–386	14–612	16–184	silicified
		4	20.72–39.15	15.32–17.57	38.30–54.10	0.45–0.79	1.24–2.00	113–592	15–211	16–477	unaltered
		8	18.76–271.18	15.78–42.40	36.13–80.86	0.16–0.84	0.15–2.85	152–1654	11–479	36–9547	desilicified
		2	39.05–139.33	18.04–28.31	56.86–62.38	0.20–0.46	0.45–1.46	170–209	226–359	403–4089	fractures
	Nungbalgarri	5	35.75–150.81	16.66–26.47	56.27–87.81	0.18–0.47	0.46–1.77	263–572	353–1813	130–6942	altered
		3	18.26–20.54	16.08–16.42	39.69–43.10	0.80–0.88	2.10–2.17	900–2782	463–642	85–166	less altered
	Mamadawerre	5	20.21–24.91	15.88–16.48	40.13–52.37	0.66–0.79	1.80–2.28	217–532	37–125	24–174	silicified
		8	20.05–23.75	15.71–16.48	40.86–50.63	0.65–0.80	1.79–2.38	277–457	24–744	18–145	unaltered
		8	20.60–40.57	15.87–17.72	39.30–56.98	0.43–0.77	1.15–2.16	147–395	44–267	27–162	desilicified

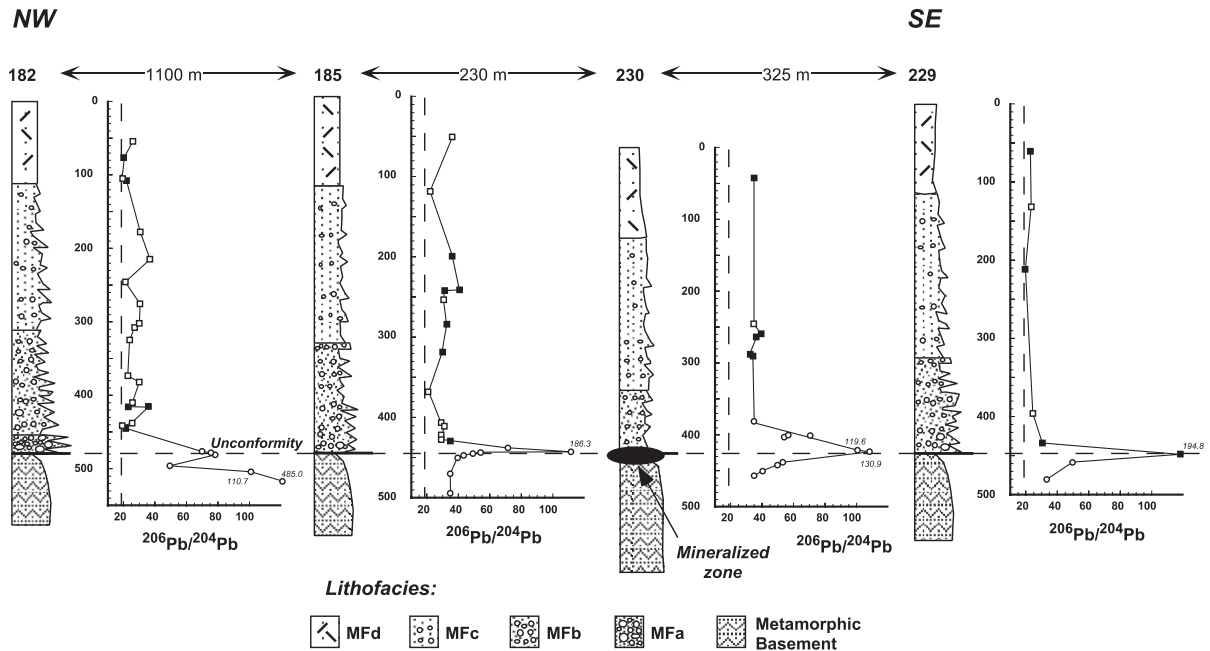


Fig. 6. Plot of $^{206}\text{Pb}/^{204}\text{Pb}$ versus stratigraphic position from drill holes proximal and distal to mineralization at Cigar Lake. Members of the Manitou Falls Formation are designated (e.g. Mfa). Data and sections are positioned such that the unconformity is at the same position. Shown are $^{206}\text{Pb}/^{204}\text{Pb}$ values from altered sandstone and basement (open dots), unaltered sandstone (solid boxes) and silicified sandstone (open boxes). The dashed line at $^{206}\text{Pb}/^{204}\text{Pb} = 18.70$ corresponds to the modern $^{207}\text{Pb}/^{206}\text{Pb}$ value for common Pb.

ty between these units (Marlatt et al., 1992). Pb–Pb ages of uraninite ore and Rb–Sr ages of coeval illite constrain the formation of the orebody at ca. 1500–1600 Ma (Kotzer and Kyser, 1993). Alteration is characterized by intense silicification of the lower 150 m of the Manitou Falls Sandstone just above the unconformity (Marlatt et al., 1992). Hydrothermal clay alteration is weak and is comprised of an early illite overprinted by late-stage kaolinite (Kotzer and Kyser, 1995). Fayek and Kyser (1997) found that chemical U–Pb ages of most late-stage Cu–U hydrates and coffinites from McArthur River were less than 195 Ma.

$^{206}\text{Pb}/^{204}\text{Pb}$, $^{207}\text{Pb}/^{204}\text{Pb}$ and $^{208}\text{Pb}/^{204}\text{Pb}$ ratios from McArthur River indicate a different late-stage fluid history from that for Cigar Lake (Fig. 7). These data are summarized in Table 3. Except for thin siltstone layers, extensive zones of silicified Manitou Falls sandstone have non-radiogenic Pb isotope ratios ($^{206}\text{Pb}/^{204}\text{Pb} = 17.64\text{--}31.00$), even within meters of the unconformity. Silicified sandstones have higher $^{206}\text{Pb}/^{204}\text{Pb}$ ratios (30.57–109.31) near the

ore zone. Except for siltstone layers and sandstones within 30 m of mineralization, all fine size fractions have non-radiogenic Pb isotope ratios. Coarse-fraction $^{206}\text{Pb}/^{204}\text{Pb}$ and $^{207}\text{Pb}/^{204}\text{Pb}$ ratios are elevated through the entire sandstone section above the deposit, indicating upward migration of mobile radiogenic Pb or U, most likely along faults. There is no apparent correlation between Pb isotope ratios and the concentration of leachable Pb. Radiogenic Pb concentrations for most sandstones are within the expected values produced from the decay of U and Th contained within these rocks, consistent with these rocks being impermeable to late-stage fluids and early U-migration. Overall, these data indicate that early-stage and syn-mineralization silicification is an effective means of isolating parts of the system from the effects of later fluid events.

5.4. The Thelon Basin

Five drill holes from the eastern Thelon Sub-basin were studied (Fig. 8). Holes DPR-9 and DPR-6 are

Table 3

Ranges in Pb isotopic compositions and concentrations of Pb, Th and U (ppm) in leachates of coarse and fine fractions of various lithologies in drill core from around the Cigar Lake deposit

Drill hole	Lithology	Number	$^{206}\text{Pb}/^{204}\text{Pb}$	$^{207}\text{Pb}/^{204}\text{Pb}$	$^{208}\text{Pb}/^{204}\text{Pb}$	$^{207}\text{Pb}/^{206}\text{Pb}$	$^{208}\text{Pb}/^{206}\text{Pb}$	Pb	Th	U
<i>Cigar Lake, Athabasca Basin</i>										
Hole 231	Sandstone	3	55.41–130.86	18.04–21.86	51.11–93.47	0.16–0.33	0.55–0.92	453–8107	452–87292	1191–135126
Hole 231	Basement	4	36.91–52.16	17.16–18.69	54.70–59.35	0.34–0.47	1.10–1.51	9437–41618	2976–3862	844–2628
Hole 182	Sandstone	21	18.36–74.21	15.63–20.70	38.93–155.92	0.28–0.88	1.08–2.63	102–1370	23–3267	35–3005
Hole 182	Basement	5	49.56–485.04	19.91–67.73	48.70–76.48	0.14–0.40	0.10–1.17	111–1164	118–3948	744–114410
Hole 230	Sandstone	9	23.49–70.18	15.47–18.86	37.24–62.09	0.27–0.66	0.88–1.73	268–5504	19–199	665–8854
Hole 230	Basement	2	37.74–41.34	17.35–17.60	57.98–58.07	0.43–0.46	1.41–1.54	7380–19583	1779–2921	2180–22762
Hole 185	Sandstone	15	21.25–40.67	15.85–18.43	39.78–294.31	0.45–0.75	1.36–7.24	140–2112	72–32631	43–834
Hole 185	Basement	8	34.26–186.35	17.16–28.35	56.73–122.81	0.15–0.50	0.66–1.97	408–7021	168–5889	185–15607
Hole 229	Sandstone	6	19.50–194.80	15.77–32.90	39.03–65.97	0.17–0.81	0.34–2.00	214–382	24–3095	33–1311
Hole 229	Basement	2	33.29–48.86	17.74–18.69	54.65–58.81	0.38–0.53	1.20–1.64	373–423	131–153	201–595
<i>MacArthur River, Athabasca Basin</i>										
RL-86	Sandstone	6	17.64–67.79	14.14–19.82	34.28–79.05	0.29–0.81	1.17–1.98	45–138	5–585	23–1425
RL-51	Sandstone	9	18.29–35.87	15.04–16.69	38.65–88.58	0.47–0.82	1.63–3.36	104–1490	14–7221	10–418
MR-222	Sandstone	4	30.57–52.64	17.75–23.16	48.73–67.00	0.44–0.67	1.28–1.71	67–1375	20–51	143–2366
MR-224	Sandstone	14	23.55–109.31	18.80–31.98	46.37–203.19	0.21–0.80	0.62–3.33	30–524	3855–8392	124–9943
<i>Thelon Basin, Nunavut</i>										
81-D-2	Sandstone	6	16.86–46.89	14.20–19.04	34.17–48.04	0.41–0.88	0.92–2.16	283–2024	23–280	49–615
80-D-2	Sandstone	4	17.98–33.25	15.98–23.32	41.77–101.77	0.70–0.90	1.83–3.06	220–703	205–1066	91–225
DPR-6	Sandstone	19	20.80–43.81	15.96–18.60	41.47–53.12	0.43–0.78	1.04–2.33	125–1326	274–14888	163–2499
DPR-9	Sandstone	6	18.86–49.94	15.54–18.56	35.70–56.40	0.37–0.82	1.06–2.30	609–11605	403–2279	245–7846
81-D-4	Sandstone	17	15.56–56.70	13.45–19.30	34.00–54.49	0.34–0.87	0.88–2.64	178–9025	52–1307	34–1323
	Basement	2	22.73–38.85	18.03–16.18	41.28–42.53	0.46–0.71	1.06–1.87	162–589	29–38	70–20488

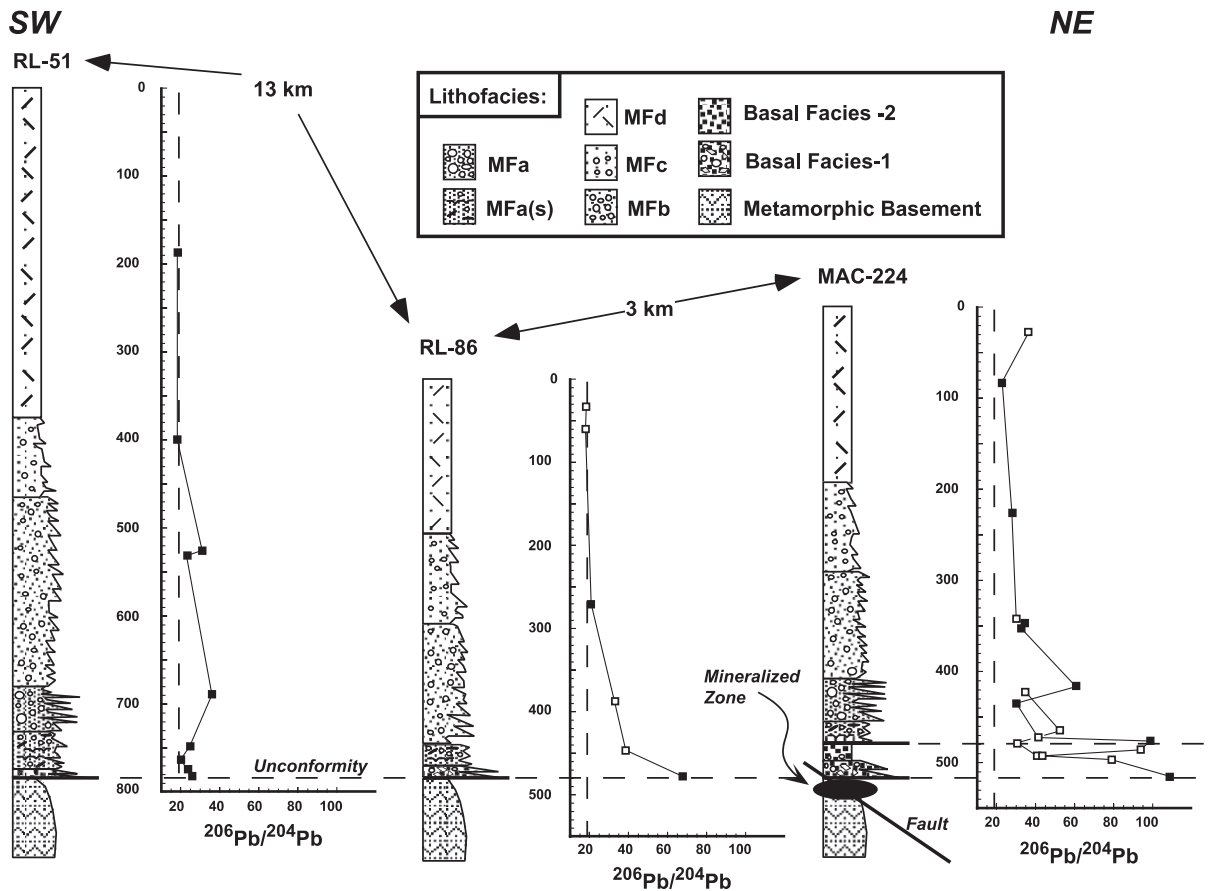


Fig. 7. Plot of $^{206}\text{Pb}/^{204}\text{Pb}$ versus stratigraphic position from drill holes proximal and distal to mineralization at McArthur River. See Fig. 6 for symbols.

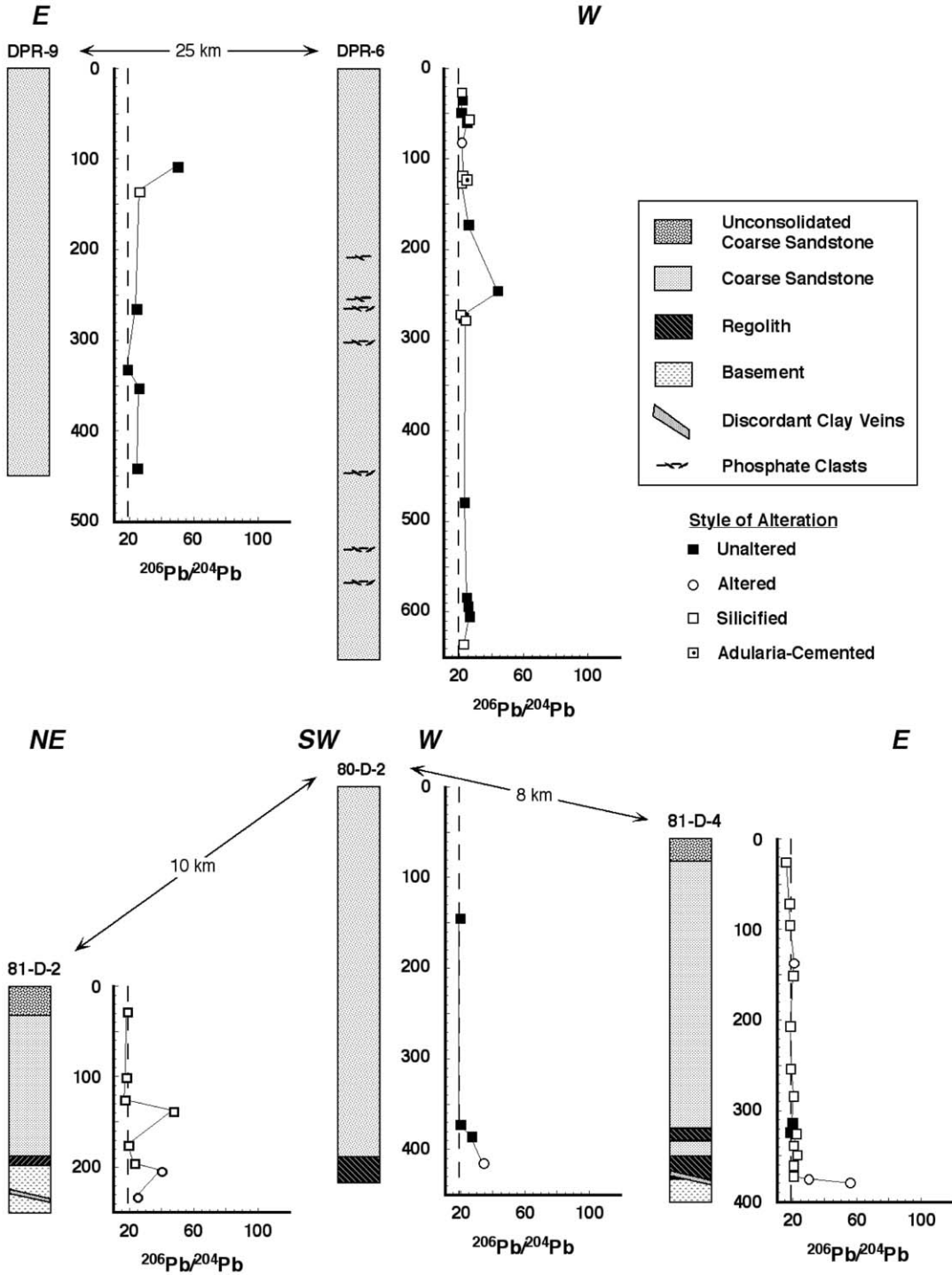
located in the central part of the sub-basin far from known mineralization (Fig. 2b). These holes sample thick sequences of Thelon Formation sandstone, but the holes did not reach the unconformity. In order to get a better understanding of basinal hydrogeology closer to mineralization, three drill holes (80-D-2, 81-D-2 and 81-D-4) that penetrate the unconformity and associated paleosols located within 15 km of the Kiggavik deposit were included (Fig. 2). Pb-isotope

and element concentration data from the Thelon Basin are summarized in Table 3.

5.4.1. Central Thelon Sub-basin

Numerous zones containing phosphate-rich clasts characterize hole DPR-6 (Fig. 8). Through 640 m of sandstone, most $^{206}\text{Pb}/^{204}\text{Pb}$ ratios are non-radiogenic (20.79–25.33), indicating minimal migration of radiogenic Pb through the section. However, leachable

Fig. 8. Plot of $^{206}\text{Pb}/^{204}\text{Pb}$ versus depth from drill holes located in the central part of the northeastern (DPR-6 and DPR-9) and the southern (81-D-2, 80-D-2 and 81-D-4) parts of the Thelon Sub-basin. The drill holes in the southern part of the basin are within 20 km of the Kiggavik uranium deposit. Denoted are altered sandstone (open dots), unaltered sandstone (solid boxes), silicified sandstone (open boxes) and adularia-cemented sandstone (dotted boxes). The dashed line at $^{206}\text{Pb}/^{204}\text{Pb}=18.700$ corresponds to the $^{206}\text{Pb}/^{204}\text{Pb}$ of common Pb. Lithologic columns from Renac et al. (2002).



U concentrations in many of these sandstones are all greater than 160 ppb, a background value much higher than that observed for other basins. One desilicified sample (DPR-6-83) contains 2499 ppb of leachable U. Only one sample at a depth of 240 m in DPR-6 has radiogenic $^{206}\text{Pb}/^{204}\text{Pb}$ ratios, and this is a conglomerate containing phosphate clasts surrounded by alteration haloes.

DPR-9 is located 25 km west–northwest of DPR-6 (Fig. 2). Sandstones in this hole have similarly low $^{206}\text{Pb}/^{204}\text{Pb}$ values (18.86–26.12) and high background leachable U concentrations (245–493 ppb). The only sample that has a radiogenic $^{206}\text{Pb}/^{204}\text{Pb}$ ratio of 49.94 also has a high uranium content of 1528 ppb. Taken as a whole, these Pb isotope data from central part of the eastern Thelon Basin indicate no migration of radiogenic Pb through this part of the basin.

5.4.2. Southeastern Thelon Sub-basin

Hole 80-D-2 is a 440-m deep hole that was drilled to the unconformity located about 20 km west of Kiggavik (Fig. 8). All of the sandstones analyzed from this locality have nonradiogenic $^{206}\text{Pb}/^{204}\text{Pb}$ ratios (17.98–26.59), but the ratios begin to increase within 20 m of the unconformity. Uranium concentrations from these sandstones are low (<120 ppb) relative to samples from the center of the basin. A silicified paleosol at the unconformity has a slightly radiogenic $^{206}\text{Pb}/^{204}\text{Pb}$ ratio (33.24) and a slightly higher leachable U concentration (225 ppb).

Drillhole 81-D-2 is 235 m in length through the heavily silicified basal Thelon Formation and is located 12 km northwest of Kiggavik. Most silicified sandstones have non-radiogenic $^{206}\text{Pb}/^{204}\text{Pb}$ ratios (18.92–22.70) and moderate leachable U concentrations (49–233 ppb). One silicified conglomerate 40 m above the unconformity has a $^{206}\text{Pb}/^{204}\text{Pb}$ value of 46.88 accompanied by a high uranium content (560 ppb), probably due to the preferential concentration of heavy minerals. A heavily altered, slightly mineralized (20488 ppb U) sheared gneiss with red hematite alteration at the unconformity has a moderately radiogenic $^{206}\text{Pb}/^{204}\text{Pb}$ ratio (38.84). Chloritic gneiss with calcite veins 30 m below the unconformity has a nonradiogenic $^{206}\text{Pb}/^{204}\text{Pb}$ ratio (22.72) and very low leachable uranium (70 ppb). This relationship in the basement indicates that, like all the previous

basins, the unconformity is a preferential site of uranium and radiogenic Pb deposition.

81-D-4 is the drill hole closest to Kiggavik at a distance of 10 km. All sandstones from this hole have $^{206}\text{Pb}/^{204}\text{Pb}$ ratios within analytical error of common Pb (17.07–24.97) yet have variable leachable uranium concentrations (53–987 ppb). Siltstones at the bottom of the section have the highest uranium concentrations (342 and 987 ppb). In the basement, $^{206}\text{Pb}/^{204}\text{Pb}$ ratios are more radiogenic (29.32 and 56.69) and these increase downward through the uppermost 5 m of basement. Leachable uranium concentrations in these gneisses are moderate (1323 and 841 ppb) relative to other basement rocks from the Thelon Sub-basin.

6. Discussion

These partial-leach Pb isotope techniques will be effective in the exploration for uranium resources only if data are considered within their geologic context. It is especially important to identify potential pathways of late-stage fluid flow prior to the employment of these isotopic and trace element techniques and to verify that the radiogenic Pb and other components that have been added to the sample do not reflect “background” values. To this end, the effects of potential reductants such as mafic volcanic rocks and the permeability history of the unconformity, fractures, faults, and silicified zones must be assessed in the area of interest. Potential point sources for Pb isotopes and mobile metals in the basin other than the deposits themselves need to be recognized. For Pb, the isotopes that are produced in situ must be accounted for (Fig. 9A–D). This will be a function of the U/Pb ratio in the sample and the time that has passed. Any excess ^{206}Pb or ^{207}Pb that could not have been produced by the amount of U in the sample must have been derived from an extraneous U-rich source, such as a uranium deposit, and then introduced into the rock by post-mineralization fluids. This excess radiogenic Pb that is not internally supported by U and Th in the rock could serve as a tracer that records the pathways and direction of late-stage fluid migration through sedimentary basins that host uranium deposits. Hence, the explorationist has much to gain by the recognition of geochemical vectors of increasingly

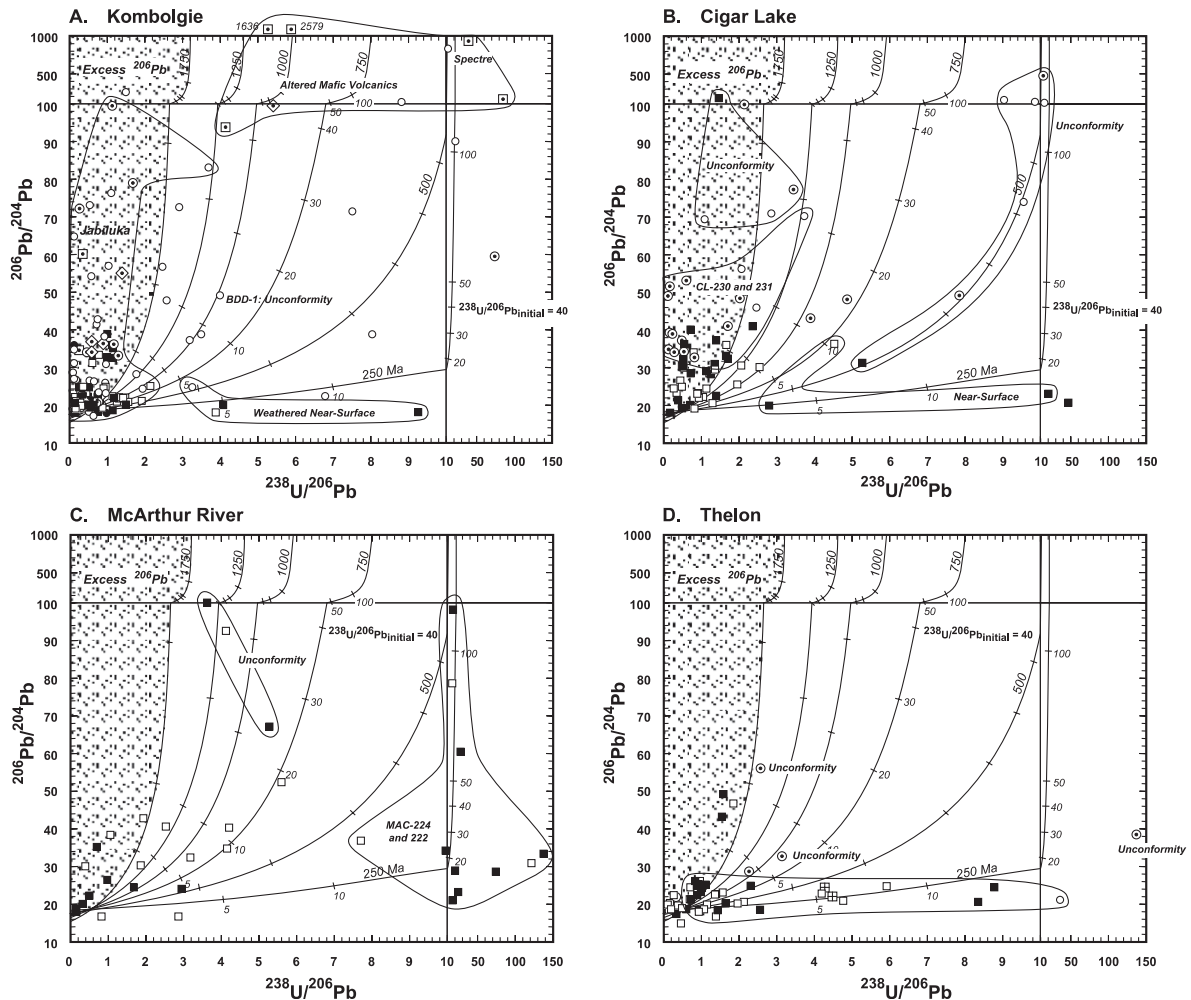


Fig. 9. Plot of $^{206}\text{Pb}/^{204}\text{Pb}$ versus $^{238}\text{U}/^{206}\text{Pb}$ showing the evolution of isotopic ratios from 1750 to 250 Ma. All samples fall into the shaded area to the left of the 1750 Ma U–Pb evolution curve are interpreted to have ^{206}Pb contents in excess of the amount of leachable uranium in the sample. Indicated on the isotopic evolution curves (at 10, 20, 30, 40, 50 and 100) are the initial $^{238}\text{U}/^{206}\text{Pb}$ ratios. (A) Data from the Kombolgie Basin. Indicated are isotopic data from basement schist and plutonic rocks (bulls-eye symbol), the Oenpelli Dolerite (dotted squares), the Nungbargari Volcanics (dotted open diamonds), silicified (quartz-cemented) sandstone (open squares), desilicified (removal of quartz) sandstone (open dots) and sandstone with clay in the matrix and few quartz overgrowths (closed squares). Field of samples from Jabiluka, weathered near-surface and altered mafic volcanic rocks are indicated. Numerous sandstones having excess ^{206}Pb are associated with fractures or are situated within 20 m of the unconformity. Except otherwise indicated, all samples with U-supported radiogenic Pb isotope ratios are either located proximal to mafic volcanic units or are from hematite-bearing fractured silicified sandstones. (B) Data from the vicinity of the Cigar Lake deposit, Athabasca Basin. Symbols are the same as (A). Indicated are the fields of data collected within 40 m from the Manitou Falls-basement unconformity, drill holes 230 and 231 that cut mineralized zones, and near-surface samples. (C) Data from the vicinity of the McArthur River deposit, Athabasca Basin. Symbols are the same as (A). Fields for samples from just above the unconformity and holes MAC-222 and 224; two holes drilled through the section above the mineralized zone are shown. (D) Isotopic results of samples from the Thelon Basin. Except for adularia-cemented sandstone (crossed open squares), all symbols are identical to (A). Highlighted are fields of data from the central Thelon Basin (drill holes DPR-6 and DPR-9), basement samples from just beneath the unconformity and conglomerates.

radiogenic Pb-isotope ratios that point toward sites of high potential for economic uranium mineralization.

6.1. Anomalous uranium at the margins of mafic volcanic units

Mafic volcanic units in the Kombolgie Basin are reductants resulting in localized uranium deposition. Oxidized basinal fluids moving through the sandstone transported U^{6+} that was reduced to U^{4+} as the fluids encountered the mafic volcanic units and reduced Fe-bearing minerals such as pyroxene, olivine and amphibole (e.g., Komminou and Sverjensky, 1996; Kyser et al., 2000). Indeed, the margins of the volcanic units in the Kombolgie Basin do have aberrantly high uranium contents, indicating that the basinal fluid was transporting U^{6+} that was fixed at the margins. Fluid compositions would have become more Ca- and Mg-rich in response to the alteration of the mafic rocks. Where the sandstones contact volcanic units in the Kombolgie, both have radiogenic Pb isotope ratios (Fig. 3) as well as high leachable Pb and U contents (Fig. 9A). The $^{238}U/^{206}Pb$ and $^{206}Pb/^{204}Pb$ ratios of these samples (Fig. 9A) are consistent with much of the radiogenic Pb being produced in situ since early diagenesis at ca. 1700 Ma or from later fluid events at ca. 1400 and 900 Ma. Thus, any basin that contains extensive interlayered mafic volcanic units would have localized enrichment of reduced uranium along the contacts if the basinal fluid were transporting U^{6+} . This localized uranium enrichment will produce radiogenic Pb, resulting in radiogenic ratios in situ or radiogenic Pb that can be mobilized by later fluids and be trapped elsewhere.

In addition to causing both local and more distal Pb isotope anomalies, the volcanic units may also affect the uranium budget of the basin. Leachable uranium concentrations measured in altered Nungbalgarri volcanic rocks within a meter of the sandstone contact average 2 ppm above background whereas the contact zones of the Oenpelli Dolerite have higher average leachable uranium enrichments of ca. 100 ppm. The Gilruth Volcanic unit is thin, but probably analogous to the Nungbalgarri volcanic rocks. All of these mafic intrusive and volcanic units occur through the entire areal extent of the basin (about 3000 km²). Using these estimates for the U enrichment in the igneous rocks as a result of interacting with a basinal brine,

there would be approximately 3×10^8 kg of uranium distributed amongst these regional-scale zones of subeconomic mineralization. According to Needham (1988), the demonstrated uranium resources of the Kombolgie Sub-Basin deposits total 5×10^8 kg. Therefore, our estimate for the total amount of uranium trapped in these volcanic units approaches the known uranium resources for the region. Existence of these mafic lithologies early in the diagenetic history of the Kombolgie Basin (e.g., Kyser et al., 2000) most likely resulted in removal of significant amount of uranium from basinal fluids and segmentation of the basin hydrogeology as it relates to the transport of uranium. Presently, these mafic units are potential sites of low-grade uranium and radiogenic Pb enrichments above normal background and sources of mobile radiogenic Pb.

6.2. Stratigraphic controls

Stratigraphy appears to affect the mobility of metals and radiogenic Pb. Sandstones that have been silicified by early quartz cementation tend to have common Pb isotopes and low leachable contents of metals. This contrasts with conglomeratic lithologies and those with clay minerals in the matrix and limited quartz cements that have radiogenic Pb isotopic compositions and elevated metal contents, especially in the environs of a known deposit. Almost all silicified sandstones have Pb isotope ratios indicative of common Pb or Pb produced in situ (open squares in Fig. 9A–D). These impermeable silicified rocks have low $^{206}Pb/^{204}Pb$ ratios and low Pb and other metal concentrations, consistent with the early isolation of these rocks from later fluid events (e.g., Kyser et al., 2000). These units served as aquitards through most of the evolution of these basins even near some large ore deposits, as indicated by the nonradiogenic character of silicified sandstone at Jabiluka (Fig. 9A), even within 10 m of the deposit (Fig. 4). At Cigar Lake, the $^{206}Pb/^{204}Pb$ ratios of silicified sandstones are generally less radiogenic than the isotopic ratios from sandstones lacking significant silica cement (Fig. 9B). Near the McArthur River deposit, few quartz-cemented sandstones show anomalous Pb isotopic compositions (Fig. 9C).

For the conglomerates, high metal contents may reflect heavy minerals such as zircon, apatite and monazite that concentrated uranium and associated

daughter Pb, if they were not altered by basinal brines. For example, the few Thelon sandstones with radiogenic $^{206}\text{Pb}/^{204}\text{Pb}$ ratios are conglomerates containing preserved heavy minerals. These samples have $^{238}\text{U}/^{206}\text{Pb}$ ratios indicative of closed system decay of U since at least 1800 Ma (Fig. 9D). The phosphatic upper part of the Thelon sequence at DPR-6 has anomalously high uranium concentrations relative to sandstones from the Athabasca and Komolgie Basins, but $^{206}\text{Pb}/^{204}\text{Pb}$ ratios are nonradiogenic. In this case, there has been recent addition of uranium (Fig. 9D), most likely from breakdown of phosphate minerals. In the Athabasca Basin, the basal older sandstone unit tends to have more radiogenic Pb isotope ratios than the overlying sandstone units, probably due to these older sandstones being silicified and retaining heavy minerals such as zircon and apatite (Fig. 9C). The majority of samples collected from near the unconformity in all basins have leachable radiogenic Pb isotopic compositions, but this Pb could have resulted from the amount of U in the sample. In fact, most have had addition of U. Hence, these apparent anomalies in Pb isotopes and metal contents reflect background enrichment at the unconformity, with the radiogenic Pb reflecting in situ production.

At the Spectre locality in the southern Komolgie Basin, silicified fault zones were closed to fluid flow very early in their history. Fault splays appear to be the site of late-stage Pb and U migration (Fig. 5). Similarly, the fault zone at U-65-2 was sealed because silicified and unaltered samples at the unconformity have non-radiogenic Pb isotopic compositions (Fig. 4). This implies that silicified sandstones, except where cut by late fractures, experience only limited degrees of late-stage fluid movement, or that there is no source of radiogenic Pb (e.g., uranium deposits) upstream along the flow path.

6.3. Fractures as avenues of fluid transport

In the Komolgie Basin, both the margins of volcanic units and drusy quartz-filled fractures that cut silicified zones near ore deposits have elevated Pb isotope ratios (Fig. 4). These fracture zones were permeable to basinal fluids and thus served as possible avenues of radiogenic Pb migration. Much of the quartz formed in these veins has been coated with

hematite and other iron oxide minerals that could have incorporated Pb either during their crystallization or adsorbed radiogenic Pb from later fluids onto their surfaces. The $^{238}\text{U}/^{206}\text{Pb}$ and $^{206}\text{Pb}/^{204}\text{Pb}$ ratios indicate migration of U and Pb into these fractures at any time between 400 and 1700 Ma (Fig. 9A). Thus, the nature (volcanic-hosted or an unconformity-type deposit?) of these anomalous uranium and radiogenic Pb occurrences can be determined.

Another example of fracture-controlled movement of radiogenic Pb and U along fractures through an intensely silicified sandstone section is just above the mineralized zone at the McArthur River deposit (Fig. 7). The radiogenic $^{206}\text{Pb}/^{204}\text{Pb}$ ratios and high $^{238}\text{U}/^{206}\text{Pb}$ ratios in these silicified rocks proximal to mineralization (<200 m) indicate episodes of U and radiogenic Pb migration at 1250 and 900 Ma (Fig. 9C), most likely along faults and fractures. Silicified sandstones with radiogenic $^{206}\text{Pb}/^{204}\text{Pb}$ ratios are also observed in the lowermost 100 m of the Manitou Falls Formation in a hole located 3 km from the mineralized zone (Fig. 7). The timing of the introduction of U into these silicified sandstones at McArthur River occurred contemporaneous with the development of secondary uranium minerals in the ore zones (e.g., Fayek and Kyser, 1997).

6.4. The permeable unconformity

Unconformities are zones of enhanced permeability in addition to serving as the boundary between oxidized basinal sandstone lithologies and reduced basement schists and volcanic rocks. Most unconformities proximal to mineralization (<1.5 km) have very radiogenic Pb isotope ratios. Our data from the Thelon Basin and the environs of the McArthur River deposit show that the scale of late-stage U and Pb migration along the unconformity is between 1.5 and 8 km (Figs. 7 and 8). The non-radiogenic $^{206}\text{Pb}/^{204}\text{Pb}$ ratio at the unconformity a few kilometers south of Nabarlek in the Komolgie Basin (Fig. 4) indicates only limited movement of late fluids along this boundary in this area. However, Pb isotope systematics of unconformity-related rocks can provide a valuable means of determining the direction of late-stage fluid flow. This is shown at Cigar Lake where the direction of fluid flow along the unconformity was most likely to the northwest, as indicated by variations

in the thickness of the zone of radiogenic Pb isotope ratios in sandstone and basement lithologies (Fig. 7), and at McArthur River with a southwest to northeast direction of fluid movement after the main stage of mineralization.

The magnitude of radiogenic $^{206}\text{Pb}/^{204}\text{Pb}$ ratios at the unconformity can be a valuable means of assessing the relative prospectivity of a given part of a basin. Sandstones and unconformity samples with $^{206}\text{Pb}/^{204}\text{Pb}$ ratios greater than 100 are all situated within 1 km of mineralization at Cigar Lake (Fig. 9B), McArthur River (Fig. 7), and Jabiluka (Fig. 4). Moderate, but still radiogenic, $^{206}\text{Pb}/^{204}\text{Pb}$ ratios near the unconformity are located as far as 8 km from known mineralized zones at the Thelon Basin (Kiggavik), Cigar Lake and McArthur River. However, paleosols typically have anomalous concentrations of U (e.g., MacDonald, 1985), so these zones would be expected to have radiogenic $^{206}\text{Pb}/^{204}\text{Pb}$ ratios at the onset of basin evolution. Unsupported $^{206}\text{Pb}/^{204}\text{Pb}$ ratios at the unconformity indicates that U has been removed or, more likely, radiogenic Pb from a U-rich source has been added.

6.5. Proximity to ore deposits in sandstones

With the exception of the altered margins of mafic volcanic units and conglomeratic samples containing heavy minerals, all sandstone sections distal to known uranium deposits have dominantly non-radiogenic Pb isotope ratios. Sandstone sections above the Jabiluka (V-258 and X-198; Fig. 4), Cigar Lake (CL-230 and CL-231; Fig. 6) and McArthur River (MR-222 and MR-224; Fig. 7) uranium deposits typically have radiogenic Pb isotope ratios. These radiogenic Pb isotopic compositions are unsupported by the amount of U in the sandstones above the Jabiluka (Fig. 9A) and Cigar Lake (Fig. 9B) deposits, consistent with the introduction of these daughter isotopes from the deposits during post-mineralization fluid events. These radiogenic $^{206}\text{Pb}/^{204}\text{Pb}$ ratios (>30) are most pronounced in the hanging wall alteration zone at Cigar Lake, where every sample from this section has elevated isotopic ratios. This heavily altered section of the Manitou Falls Formation lacks any silicified zones, so it was permeable to late fluids through its entire thickness. This contrasts with the data from McArthur River and Jabiluka, where the presence of

the impermeable silicified zones above the deposits retarded late-stage migration of radiogenic Pb and U. However, fracturing of the silicified sandstones above the McArthur River deposit facilitated the introduction of radiogenic Pb and U during and following mineralization whereas these fluids only infiltrated along fault splays at the Spectre locality in the Kombolgie Basin.

7. Conclusions

Studies of Pb isotopes and mobile trace elements from weak acid leaching of basement rocks and basin sediments provide insight into the late-stage fluid history of Proterozoic sedimentary basins that host unconformity-type uranium deposits. Early isolation of silicified zones from basinal fluids preclude these lithologies as being useful for determining modes of post-mineralization element transport. Radiogenic Pb in mafic volcanic rocks indicate these served as local sinks of U during diagenesis. The presence of such volcanic rocks in a basin hinders the formation of large deposits at the unconformity due to the scavenging of uranium from the basinal fluids prior to their reaching the unconformity. Late structures, such as fractures and faults, were the most likely avenues of late-stage element migration in these basins; thus, these domains within a basin have the greatest utility for determining whether anomalous concentrations of uranium are present along the upstream path of these structures.

Acknowledgements

The authors would like to thank research colleagues and the laboratory staff at Queen's University geochemical laboratories for valuable discussion and laboratory assistance. These include Paul Polito, Kyle Durocher, Kerry Klassen, Aliona Valiashko, Sarah Palmer, Andrew Bukata, Nancy Norton and Olivia Gibb. We also thank the staff at Cameco, most notably Vlad Sopuck, Garth Drever, Dave Thomas and Ted O'Connor for providing logistical, technical and geological assistance and advice. This project was funded by NSERC, Cameco and Uranerz Collaborative Research and Development, NESRC operating,

equipment and CRD grants to TKK, and a grant from the Geological Survey of Canada.

References

- Armstrong, R.L., Ramaekers, P., 1985. Sr isotopic study of Helikian sediment and diabase dikes in the Athabasca Basin, northern Saskatchewan. *Canadian Journal of Earth Sciences* 22, 399–407.
- Baadsgaard, H., Cumming, G.L., Worden, J.M., 1984. U–Pb geochronology of minerals from the Midwest uranium deposit, northern Saskatchewan. *Canadian Journal of Earth Sciences* 21, 642–648.
- Binns, R.A., McAndrew, J., Sun, S.S., 1980. Origin of uranium mineralization at Jabiluka. In: Ferguson, J., Goleby, A.B. (Eds.), *Proceedings of the International Uranium Symposium on the Pine Creek Geosyncline*. International Atomic Energy Agency, Vienna, pp. 543–562.
- Bruneton, P., 1993. Geological environment of the Cigar Lake deposit. *Canadian Journal of Earth Sciences* 30, 653–673.
- Cameco Corporation, 1997. Annual Report.
- Donnelly, T.H., Ferguson, J., 1980. A stable isotope study of three deposits in the Alligator Rivers uranium field, Northern Territory. In: Ferguson, J., Goleby, A.B. (Eds.), *Uranium in the Pine Creek Geosyncline*, Proceedings Series. International Atomic Energy Agency, Vienna, pp. 397–406.
- Durak, B., Pagel, M., Poty, B., 1983. Temperatures et salinités des fluides au cours de la silicification diagenétique d'une formation gréseuse surmontant un gisement d'uranium du sicle: l'exemple des gres Kombolgie (Australie). *Acad. Sci. (Paris) Comptes Rendus, Ser. 2* (296), 571–574.
- Fayek, M., Kyser, T.K., 1997. Characterization of multiple fluid-flow events and rare-earth-element mobility associated with formation of unconformity-type uranium deposits in the Athabasca Basin, Saskatchewan. *Canadian Mineralogist* 35, 627–658.
- Fouques, J.P., Fowler, M., Knipping, H.D., Schimann, K., 1986. The Cigar Lake uranium deposit: discovery and general characteristics. In: Evans, E.L. (Ed.), *Uranium Deposits of Canada*. The Canadian Institute of Mining and Metallurgy, Special Volume, vol. 33, pp. 218–229.
- Gall, Q., 1994. The Proterozoic Thelon paleosol, NWT, Canada. *Precambrian Research* 68, 114–137.
- Gandhi, S.S., 1989. Geology and uranium potential of the Thelon Basin and adjacent basement in comparison to the Athabasca Basin region. *Uranium Resources and Geology of North America*, Proceedings of a Technical Meeting of the IAEA, Saskatoon, Canada, pp. 411–427.
- Goldberg, I.S., 1998. Vertical migration of elements from mineral deposits. *Journal of Geochemical Exploration* 61, 191–202.
- Gulson, B.L., Mizon, K.J., 1980. Pb isotope studies at Jabiluka. In: Ferguson, J., Goleby, A.B. (Eds.), *Proceedings of the International Uranium Symposium on the Pine Creek Geosyncline*. International Atomic Energy Agency, Vienna, pp. 439–455.
- Gustafson, L.B., Curtis, L.W., 1983. Post-Kombolgie metasomatism at Jabiluka, Northern Territory, Australia, and its significance in the formation of high-grade uranium mineralization in lower Proterozoic rocks. *Economic Geology* 78, 26–56.
- Hall, G.E.M., 1998. Analytical perspective on trace element species of interest in exploration. *Journal of Geochemical Exploration* 61, 1–19.
- Hills, J.H., Richards, J.R., 1976. Pitchblende and galena ages in the Alligator Rivers region, Northern Territory, Australia. *Mineralium Deposita* 11, 133–154.
- Komninou, A., Sverjensky, D.A., 1996. Geochemical modeling of the formation of an unconformity-type uranium deposit. *Economic Geology* 91, 590–606.
- Kotzer, T.G., Kyser, T.K., 1991. Retrograde alteration of clay minerals in uranium deposits: radiation catalyzed or simply low-temperature exchange? *Chemical Geology* 86, 307–321.
- Kotzer, T.G., Kyser, T.K., 1993. O, U, and Pb isotopic and chemical variations in uraninite: implications for determining the temporal and fluid history of ancient terrains. *American Mineralogist* 78, 1262–1274.
- Kotzer, T.G., Kyser, T.K., 1995. Petrogenesis of the Proterozoic Athabasca Basin, northern Saskatchewan, Canada, and its relation to diagenesis, hydrothermal uranium mineralization and paleohydrogeology. *Chemical Geology* 120, 45–89.
- Kyser, T.K., Hiatt, E., Renac, C., Durocher, K., Holk, G., Deckart, K., 2000. Diagenetic fluids in Paleo- and Meso-Proterozoic sedimentary basins and their implications for long protracted fluid histories. In: Kyser, K. (Ed.), *Fluids and Basin Evolution*, Mineralogical Association of Canada Short Course Series, vol. 28, pp. 225–262.
- Lewry, J.F., Sibbald, T.I.I., 1980. Thermotectonic evolution of the Churchill Province in northern Saskatchewan. *Tectonophysics* 68, 45–82.
- Ludwig, K.R., Frauch, R.I., Nutt, C.J., Frishman, D., Simmons, K.R., 1987. Age of uranium mineralization at the Jabiluka and Ranger deposits, Northern Territory, Australia: new U–Pb isotope evidence. *Economic Geology* 82, 857–874.
- Maas, R., 1989. Nd–Sr isotope constraints on the age and origin of unconformity-type uranium deposits in the Alligator Rivers uranium field, Northern Territory, Australia. *Economic Geology* 84, 64–90.
- MacDonald, C.C., 1985. Mineralogy and geochemistry of the sub-Athabasca regolith near Wollaston Lake. In: Sibbald, T.I.I., Petruk, W. (Eds.), *Geology of Uranium Deposits*. Canadian Institute of Mining and Metallurgy, Special Volume, vol. 32, pp. 155–158.
- Mann, A.W., Birrell, R.D., Mann, A.T., Himphreys, D.B., Perdrix, J.L., 1998. Application of the mobile metal ion technique to routine geochemical exploration. *Journal of Geochemical Exploration* 61, 87–102.
- Marlatt, J., McGill, B., Matthews, R., Sopuck, V., Pollock, G., 1992. The discovery of the McArthur River uranium deposit, Saskatchewan, Canada. *New Developments in Uranium Exploration, Resources, Production, and Demand*, Proceedings of a Technical Committee Meeting Jointly Organized by the International Atomic Energy Agency and Nuclear Energy Agency of the organization for Economic Cooperation Development, Vienna, 26–29 August 1991, IAEA-TECDOC-650, pp. 118–127.
- Miller, A.R., 1983. A progress report: Uranium–phosphorous asso-

- ciation in the Helikian Thelon Formation and sub-Thelon saprolite, central district of Keewatin. Geological Survey of Canada, 449–456 (Paper 83-1A).
- Miller, A.R., LeCheminant, A.N., 1981. Geology and uranium metallogeny of Proterozoic supracrustal successions, central District of Keewatin, Northwest territories. In: Evans, E.L. (Ed.), Uranium Deposits of Canada. Canadian Institute of Mining and Metallurgy, Special Volume, vol. 33, pp. 263–285.
- Miller, A.R., Cumming, G.L., Krstic, D., 1989. U–Pb, Pb–Pb, and K–Ar isotopic study and petrography of uraniferous phosphate-bearing rocks in the Thelon Formation, Dubawnt Group, Northwest territories, Canada. Canadian Journal of Earth Sciences 26, 867–880.
- Needham, R.S., 1988. Geology of the Alligator Rivers uranium field, Northern Territory. BMR Bulletin 224 (96 pp.).
- Needham, R.S., Stuart-Smith, P.G., Page, R.W., 1988. Tectonic evolution of the Pine Creek Inlier, Northern Territory. Precambrian Research 40/41, 543–564.
- Nutt, C.J., 1989. Chloritization and associated alteration at the Jabiluka unconformity-type uranium deposit, Northern Territory, Australia. Canadian Mineralogist 27, 41–58.
- Page, R.W., Williams, I.S., 1988. Age of the Barramundi Orogeny in northern Australia by means of ion microprobe and conventional U–Pb zircon studies. Precambrian Research 40–41, 21–36.
- Page, R.W., Compston, W., Needham, R.S., 1980. Geochronology and evolution of the late-Archean basement and Proterozoic rocks in the Alligator Rivers uranium field, Northern Territory, Australia. In: Ferguson, J., Goleby, A.B. (Eds.), Proceedings of the International Uranium Symposium on the Pine Creek Geosyncline. International Atomic Energy, Vienna, pp. 39–68.
- Pagel, M., Michard, A., Juteau, M., Turpin, L., 1993. Sm–Nd, Pb–Pb, and Rb–Sr systematics of the basement in the Cigar Lake area, Saskatchewan, Canada. Canadian Journal of Earth Sciences 30, 731–742.
- Philipe, S., Lancelot, J.R., Clauer, N., Pacquet, A., 1993. Formation of the Cigar Lake uranium deposit based on U–Pb and K–Ar isotope systematics. Canadian Journal Earth Science 30, 720–730.
- Ramaekers, P., 1981. Hudsonian and Helikian basins of the Athabasca region, northern Saskatchewan. In: Campbell, F.H.A. (Ed.), Proterozoic Basins of Canada, Geological Survey of Canada, pp. 219–233. Paper 81-10.
- Rawlings, D.J., Page, R.W., 1999. Geology, geochronology and emplacement structures associated with the Jimbu Microgranite, McArthur Basin, Northern Territory. Precambrian Research 94, 225–250.
- Renac, C., Kyser, T.K., Durocher, K., Dreaver, G., O'Connor, T., 2002. Comparison of diagenetic fluids in the Proterozoic Thelon and Athabasca Basins, Canada: implications for long protracted fluid histories in stable intracratonic basins. Canadian Journal of Earth Sciences 39, 113–132.
- Ruzicka, V., 1995. Unconformity-associated uranium. In: Eckstrand, O.R., Sinclair, W.D., Thorpe, R.I. (Eds.), Geology of Canadian Mineral Deposit Types. Geological Society of America, Decade of North American Geology D-1, pp. 197–210.
- Stacey, J.S., Kramers, J.D., 1975. Approximation of terrestrial Pb isotope evolution by a two-stage model. Earth and Planetary Science Letters 26, 207–221.
- Sweet, I.P., Brakel, A.T., Carson, L., 1999. The Kombolgie Subgroup—a new look at an old ‘formation’. AGSO Research Newsletter 30, 26–28.
- Trocki, L.K., Curtis, D.B., Gancarz, A.J., Banar, J.C., 1984. Ages of major uranium mineralization and Pb loss in the Key Lake uranium deposit, northern Saskatchewan, Canada. Economic Geology 79, 1378–1386.
- Von Gunten, H.R., Roessler, E., Lowson, R.T., Reid, P.D., Short, S.A., 1999. Distribution of uranium and thorium series radionuclides in mineral phases of a weathered transect of a uranium ore body. Chemical Geology 160, 225–240.
- Wilde, A.R., Mernagh, T.P., Bloom, M.S., Hoffman, C.F., 1989. Fluid inclusion evidence on the origin of some Australian unconformity-related uranium deposits. Economic Geology 85, 1627–1642.
- Wilson, M.R., Kyser, T.K., Mehnert, H.H., Hoeve, J., 1987. Changes in the H–O–Ar isotopic composition of clays during retrograde alteration. Geochimica et Cosmochimica Acta 51, 869–878.